Preparation of Functional Microparticles and Microcapsules by Layer-by-layer Adsorption of Polyelectrolytes

Fujii, Akihiro

(Degree)
博士（工学）

(Date of Degree)
2011-03-25

(Date of Publication)
2011-10-17

(Resource Type)
doctoral thesis

(Report Number)
甲5245

(URL)
https://hdl.handle.net/20.500.14094/D1005245

Doctoral Dissertation

Preparation of Functional Microparticles and Microcapsules by Layer-by-layer Adsorption of Polyelectrolytes

（高分子電解質の交互吸着法を用いた機能性微粒子の作製）

January 2011

Graduate School of Engineering
Kobe University

Akihiro Fujii

Acknowledgement

First of all, I would like to express my deep and sincere gratitude to Professor Dr. Hideto Matsuyama for the support and the opportunity to perform my PhD study under his supervision. His advices, invaluable discussions, and teaching helped me to gain new perspectives and inspired me to undertake this challenge. I will never forget his encouragement over the years.

I am deeply grateful to Dr. Tatsuo Maruyama and Dr. Yoshikage Ohmukai, for their kind support in the laboratory and helpful discussions during this research. I sincerely thank Professor Dr. Atsunori Mori and Professor Dr. Satoru Nishiyama for their kindness during the reviewing and examining of this thesis and giving many constructive comments to make it better. I would like to extend my thanks to Dr. Tomohiro Sotani for his technical support throughout this work. Many thanks extend to all the members of Professor Matsuyama's Laboratory for assistance in many ways. I would also like to express my gratitude to my scholarship provider, Research Organization for Membrane and Film Technology, for financing my studies.

Finally, I would like to express special thanks to my parents for their understanding and cooperation. Without their mental and financial support, I would not have accomplished my PhD thesis.

Akihiro Fujii

Graduate School of Engineering

Kobe University, 2011.

Table of Contents

Chapter III Cross-linked DNA capsules templated on porous calcium carbonate microparticles

Chapter IV Preparation of DNA hydrogel capsules cross-linked through NeutrAvidin–biotin interaction

Chapter I

General Introduction

I.1 Layer-by-layer assembly technique

I.1.1 Polyelectrolyte complexes

Charged polymers, polyelectrolytes, which have positive or negative charges in water, form complex with oppositely charged polyelectrolytes or with oppositely charged surfactants [1]. Upon mixing the aqueous solutions of polycations and that of polyanions, one can usually find that the turbidity of the solutions takes place and polyelectrolyte complexes are formed. Polyelectrolytes are surrounded by low molecular weight counterions in water. The linkages of polyelectrolyte complexes are formed by the attraction between charged groups of polyelectrolytes simultaneously with the release of counter ions to the solvent. The reaction of a polyelectrolyte complex with monovalent salts can be described by the following equilibrium [1]

$$(Pol^{+}A^{-})_m + (Pol^{-}C^{+})_n \Leftrightarrow (Pol^{+}Pol^{-})_x + (Pol^{+}A^{-})_{m-x} + (Pol^{-}C^{+})_{n-x} + xA^{-}_{aq} + xC^{+}_{aq} \qquad (1)$$

where Pol^{+} and Pol^{-} are the charged groups of polycations and polyanions, respectively, A^{-} and C^{+} are counterions, the subscript m and n are the number of repeating units for the polyelectrolytes, and x is the number of ion pairs in the polyelectrolyte complex. Equation (1) indicates that the concentration of the ion pairs in the complex is influenced with the salt concentration in a solution. In addition, it indicates that the charges of polyelectrolytes forming complexes are compensated (balanced) by either the

opposite charges of polyelectrolytes or salt ions, as shown in Fig. I.1. The former case is termed “intrinsic charge compensation” and the latter is termed “extrinsic charge compensation” [2]. The more detailed schematic illustration of the formation of polyelectrolyte complex is shown in Fig. I.2. Intrinsic sites mean the polyelectrolyte/polyelectrolyte ion pairs in the complex, that is, cross-linking portions. Extrinsic sites mean polyelectrolyte/salt ion pairs in the complex, and they are considered to be divided into further three types, such as doping, trapped doping, and non-stoichiometric extrinsic sites. Doping sites are reversible between intrinsic and extrinsic charges depending on the salt concentration, as shown in Eq. (1). Whereas, trapped doping sites where the charges of polyelectrolytes are sterically constrained cannot pair with opposite polyelectrolyte charges. Non-stoichiometric extrinsic sites arise because one component is present in excess in the complex [3]. This non-stoichiometry leads to overcharging of polyelectrolyte complexes [1].

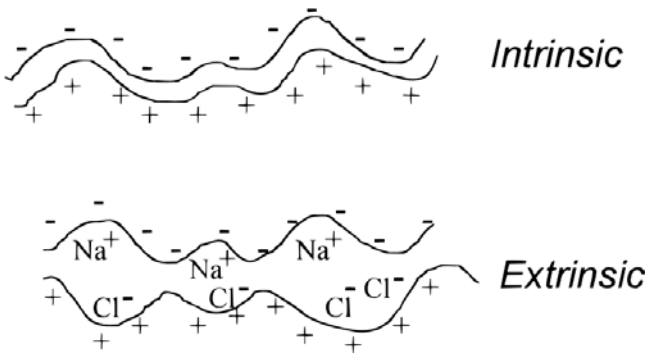

Fig. I.1 Comparison of intrinsic and extrinsic charge compensation [2].

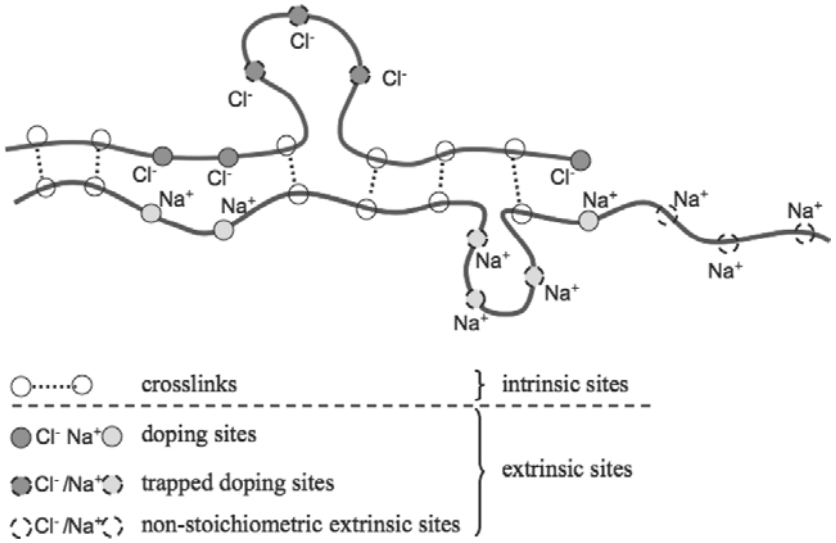

Fig. I.2 Schematic illustration of a polyelectrolyte complex and interactions [3].

I.1.2 Layer-by-layer assemblies of polyelectrolytes

Polyelectrolyte complexes can be also formed on planar substrates. In the early 1990s, Decher and co-workers developed the preparation technique of thin films comprised of polyelectrolytes, the so-called layer-by-layer (LbL) method [4,5]. By using this method, polyelectrolyte multilayer films can be deposited onto the surface of planar organic and inorganic substrates [6-8]. Fig. I.3 shows the schematic illustration of the polyelectrolyte film deposition process. The substrates, which possess a net positive charge, are initially immersed into polyanion solutions (step 1), and then are washed with water to remove the excess polyelectrolytes (step 2). The polyanion-coated substrates are successively coated with polycations, and then washed by immersion in water (step 4). By repeating these steps, polyelectrolyte multilayers are obtained on the substrates. After the adsorption of polyelectrolytes, overcompensation occurs near the surface owing to the extrinsic sites (Fig. I.2), which leads to a surface charge reversal and allows the additional adsorption of oppositely charged polyelectrolytes on the

surface [9]. The reversal of the surface charge during the LbL adsorption is followed by zeta potential measurements, and the multilayer buildup can be confirmed [10]. Multilayer buildup is also monitored by UV/VIS spectroscopy, quartz crystal microbalance, surface plasmon resonance, and X-ray reflectometry [4,5,11].

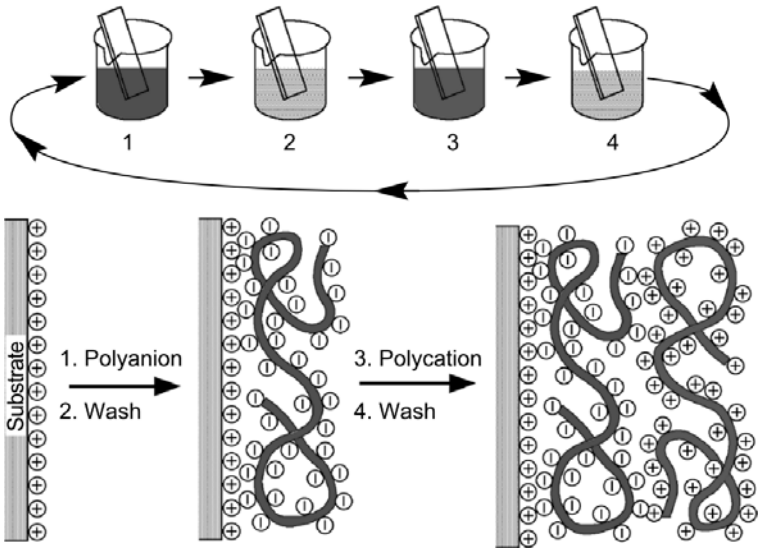

Fig. I.3 Schematic illustration of the layer-by-layer process [4].

The LbL technique provides a facile method to prepare ultrathin polymer films because polyelectrolyte multilayers can be prepared by using only beakers and tweezers. The major advantages of the LbL method are that diverse materials can be incorporated into multilayers and that the architecture of multilayers is controlled by the deposition sequence [4]. The commonly used polycations and polyanions are summarized in Fig. I.4. Alternatively, biomacromolecules such as proteins and polynucleotides [12-14] and inorganic materials such as carbon nanotubes and montmorillonites [15,16] have been employed as the components in the LbL films. So far, most of the multilayers have been prepared by using electrostatic attraction, however, that is not always necessary as a driving force for the adsorption. Besides electrostatic interaction, hydrogen bonding,

covalent bonding, charge-transfer interaction, and host–guest interaction have been used successfully for the buildup of multilayers [17-21]. This fact expands the selection of materials available for the components in multilayers.

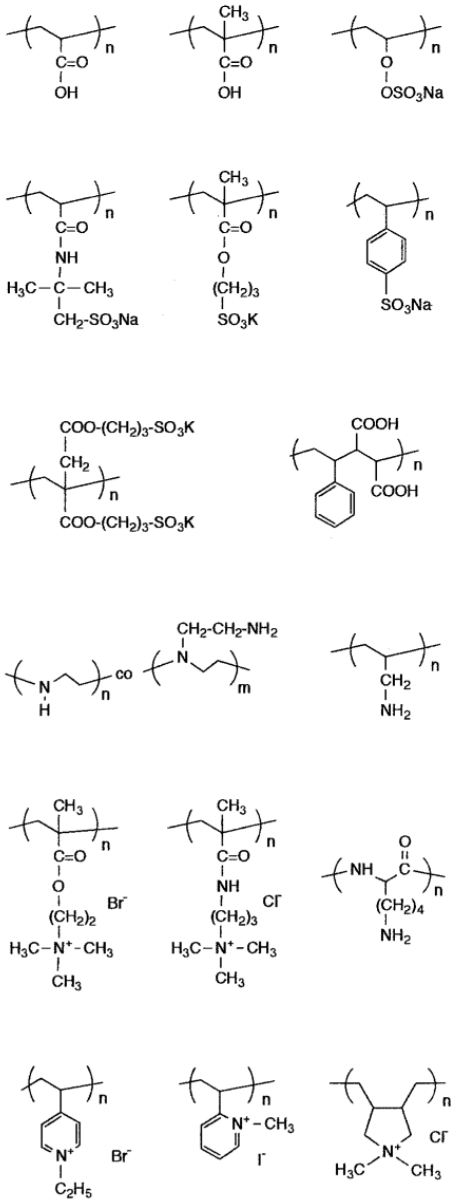

Fig. I.4 Structures of representative polyelectrolytes [6].

I.1.3 Effect of preparation condition of layer-by-layer multilayers

The thickness of LbL multilayers is easily controlled by the times of the deposition of polymers [22]. Moreover, the thickness is dependent on environmental conditions such as ionic strength and pH. The conformation of adsorbed polyelectrolytes on a substrate surface is generally described in three different types: train, loop, and tail (Fig. I.5). In train–loop–tail model, "train" indicates the most constrained segments adsorbed on a substrate surface, "loop" indicates the constrained segments surrounded by solvents between two neighboring train segments, and "tail" indicates the less constrained segments of the termination of polyelectrolyte chains [23].

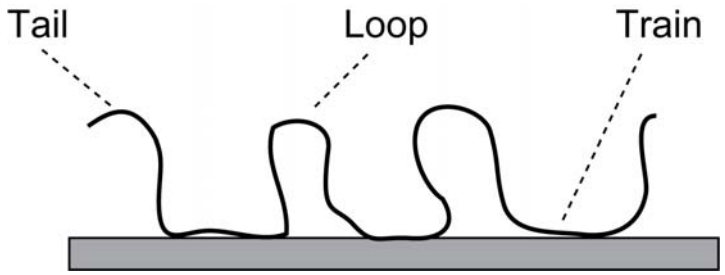

Fig. I.5 Schematic illustration of adsorbed polymers on substrates (train–loop–tail model).

I.1.3.1 Influence of salt concentration on the preparation of LbL multilayers.

In polyelectrolyte multilayers, the loop and tail segments correspond to extrinsic sites in polyelectrolyte complexes as shown in Fig. I.2. Thus, the concentration of loop segments is dependent on the concentration of salts in polyelectrolyte solutions during the preparation of multilayers. For the preparation of polyelectrolyte multilayers, substrates are usually washed with solvents before additional polyelectrolyte adsorption. However, the loop segments are considered as trapped doping sites, which are not reversible between intrinsic and extrinsic sites (Fig. I.2). The concentration of loop

segments of the top of polyelectrolyte multilayers is concerned with the density of the surface charge of multilayers. In other words, this indicates that the concentration of salts influences the adsorption amount of polyelectrolytes in the consecutive adsorption.

The influence of salt concentration in polyelectrolyte solutions on the thickness of polyelectrolyte multilayers has been studied by Dubas et al [9]. Fig. I.6 shows the thickness of multilayers prepared with polyelectrolyte solutions containing various concentrations of NaCl. This plot also shows the effect of pH and polyelectrolyte molecular weight on the thickness, as will be described below. In the case of polyelectrolyte multilayers containing strong polyacid, e.g. poly(styrene sulfonate) (PSS), the thickness of multilayers is proportional to the concentration of salts. This is because the increase of loop segments and high adsorption of polyelectrolytes with opposite charge, as described above. In the case of multilayers containing weak polyacid, such as poly(acrylic acid), although the thickness of multilayers increased in low salt concentration, the multilayers become thinner and eventually they were not formed in high salt concentrations. The polyelectrolyte complexes composed of weak polyacids are expected to have relatively weak interactions and are easily swollen owing to the ion exchange with small ions. The resulting decrease of polymer/polymer ion pairs in complexes induces less adsorption of polyelectrolytes. Furthermore, when the successfully prepared polyelectrolyte multilayers composed of weak polyacids are immersed in a solution with high ionic strength, the decomposition of multilayers would be observed. In contrast, although the multilayers prepared with strong polyacids have high salt resistance and can be prepared in high salt concentrations, the thickness variation with ionic strength is lower because of low swelling caused by strongly interaction between polyelectrolytes.

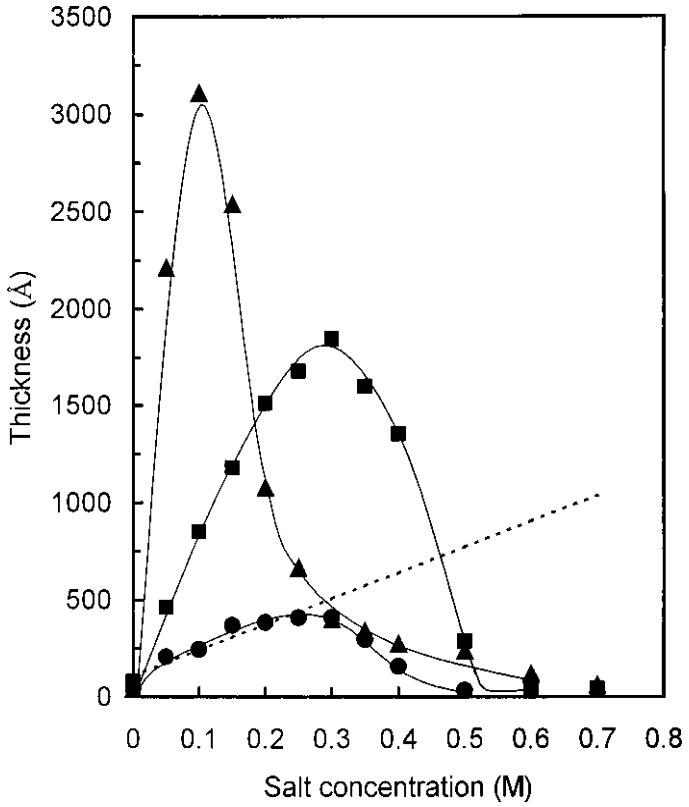

Fig. I.6 Thickness of 20-layer LbL multilayers of poly(acrylic acid) (PAA) and poly(diallyldimethylammonium chloride) (PDADMA) deposited in various NaCl concentrations. Squares: PAA (*M*r = 84,500), deposited at pH 11. Circles: PAA (*M*r = 5200), pH 11. Triangles: PAA (*M*r = 5200), pH 5. Dotted line: 20-layer multilayers of poly(styrenesulfonate) and PDADMA [9].

I.1.3.2 Influence of pH on the preparation of LbL multilayers.

The pH of polyelectrolyte solutions during the preparation affects the thickness of multilayer in the case of multilayers containing weak polyelectrolytes, i.e., weak polyacids and weak polybases. Shiratori and Rubner have intensively studied the pH-dependent thickness of polyelectrolyte multilayers consisted with poly(acrylic acid) (PAA) and poly(allylamine hydrochloride) (PAH) [24]. Figure I.7 shows the average

incremental thickness of each adsorbed polyelectrolytes. Both weak polyelectrolyte solutions were deposited on substrates with same pH and without additional salts. The ionization degree of PAA and PAH change in the pH range from 2.5 to 9. PAA chains possess a low degree of ionization at acidic pH (20–30% at pH 2.5) and are almost completely charged at and above pH 6.5. PAH chains bear positive charges in this pH range but start to be deprotonated above around pH 7.0.

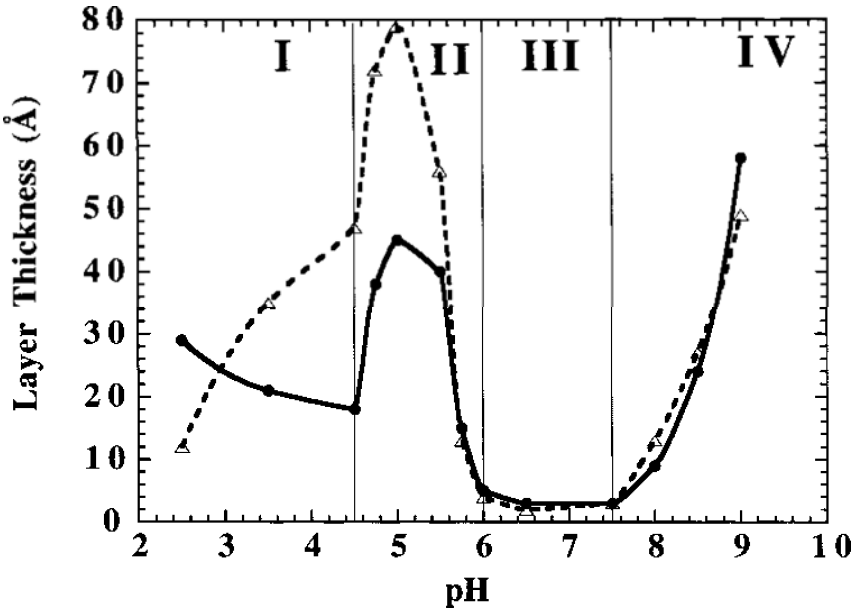

Fig. I.7 Average incremental thickness of adsorbed layer of PAA (*M*w = 90,000) PAH (*M*w = 55,000–65,000) as a function of pH. Solid and dashed lines represent the thickness of PAA and PAH layers, respectively [24].

Figure I.7 clearly indicates that the thickness of multilayers consisted with weak polyelectrolytes are very sensitive to the small changes in solution pH. Especially at pH 5.0 and 9.0, a dramatic increase of the thickness occurs. In these pH regions, to reach a high thickness per one layer, adsorbed polyelectrolytes are assumed to adopt a conformation where the loop and tail segments of polyelectrolytes are predominantly present. PAH is fully charged and PAA is close to fully charged at pH 5.0, while PAH is close to fully charged and PAA is fully charged at pH 9.0. Thus, when fully charged polyelectrolytes are adsorbed onto a layer of nearly fully charged polyelectrolytes, and vice versa, much thicker multilayers can be finally obtained. In addition, with atomic force microscopy, it was found that the surface roughness of dried multilayers prepared in region II and IV was dependent on the thickness. The surface comprised mainly of loop and tail segments will produce a molecularly rough surface, whereas that comprised mainly of train segments will produce a molecularly smooth surface [24]. The high roughness observed at pH 5.0 and pH 9.0 indicates that the adsorbed layers of polyelectrolyte segments presumably dominated largely loops and tails.

At neutral pH in region III (pH 6.0–7.5), when both polyelectrolytes are fully charged, very thin multilayers are formed. Shiratori and Rubner also demonstrated that the thickness was independent of the molecular weight of the adsorbing polyelectrolytes over a range from 3000 to 1,000,000 [24]. This result evidences that fully charged polyelectrolytes are adsorbed in an extended conformation without loops and tails on the surface as long as the multilayers are prepared from salt-free polyelectrolyte solutions. In fact, the surface roughness of the multilayers prepared in region III was very low. This result agrees with the assumption that adsorbed polyelectrolytes adopting a train conformation will provide a flat surface.

In region I (pH 2.5–4.5), the thickness of a layer of PAA increases with decreasing pH whereas that of PAH decreases with decreasing pH. This result is due to the change of the charge density of PAA chains in this pH region. Because the negative charge density of PAA decreases at more acidic pH, less PAH chains are adsorbed to compensate the charge of PAA chains, resulting in decreasing the thickness of a PAH layer. The increase of the thickness of a PAA layer with decreasing pH is considered to be related to a reduction of electrostatic repulsion within an adsorbing PAA chain [25]. At acidic pH, adsorbed PAA chains would prefer to adopt not an extended conformation but the conformation of loops and tails. In Fig. I.6, the thickness of PAA/PDADMA multilayers prepared from pH 5 solutions is greater than that prepared from pH 11 over the entire range of the tested salt concentrations. This is because partially charged PAA chains deposited at pH 5 further produce the loop and tail segments in the multilayer system.

I.1.3.3 Influence of polyelectrolyte molecular weight on the preparation of LbL multilayers.

As described above, the thickness of LbL polyelectrolyte multilayers is independent to the molecular weight of polyelectrolytes without the segments of loop and tail. The adsorbed amount of polyelectrolytes as a function of molecular weight has been experimentally demonstrated [26]. Fig. I.8 shows the adsorption amount of PSS with various molecular weights on polyoxymethylene crystals. At low ionic strength (0.53 M), because of the adsorption in a mainly flat conformation, a clear effect of the molecular weight is not found. As the ionic strength becomes higher, the dependence of the adsorbed amount with the molecular weight becomes more distinct. Considering the

results concerning the thickness from Fig. I.6 and the adsorbed amount from Fig. I.8, at high ionic strength, the adsorbed polyelectrolytes with long chains may adopt a conformation with longer loops and tails.

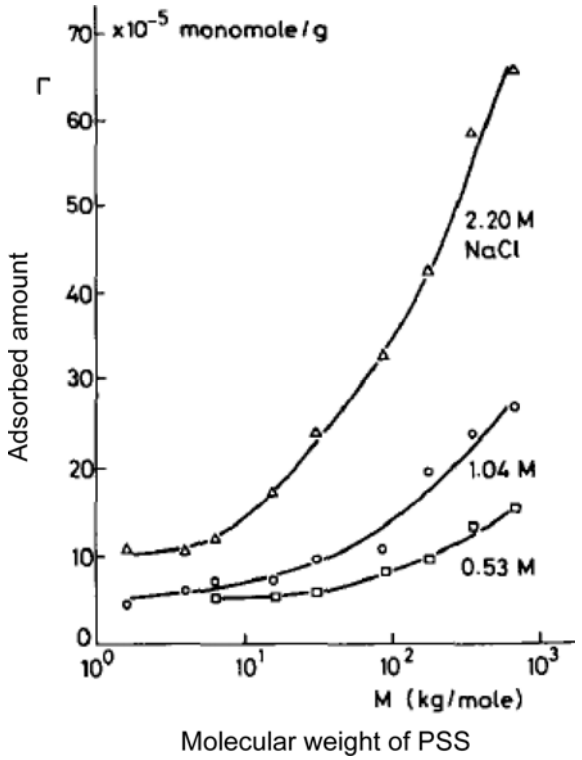

Fig. I.8 Adsorbed amount of PSS on polyoxymethylene crystals as a function of molecular weight, at three NaCl concentrations [27].

In conclusion, the preparation conditions such as the concentration of salt and pH of solutions affect the concentration of loops and tails, resulting in the preparation of thickness-controlled multilayer films. Owing to availability and facility of LbL method, the LbL multilayers have many potential applications including surface modifications such as antifouling, antibacterial coatings, and cell adhesion [28], biosensing, water treatment membrane, and pervaporation [8,20,29].

I.2 Microcapsules

I.2.1 Capsules for drug delivery applications

The study of drug carriers for drug delivery system has been extensively studied so far [30-32]. The goal of drug delivery system is to enhance the performance of drugs while preventing the side effects. To optimize the delivery of drugs, multi-functional properties, such as accurate dosing, targeting, and high stability, are necessary. However, since small drug molecules themselves cannot perform the above functions simultaneously, drugs are needed to be immobilized on or be encapsulated in functional carriers such as capsules.

The carriers used in the human body have to be composed of the materials with low cytotoxicity against human tissues and cells. Biomaterials that are biocompatible and biodegradable are appropriate to use in the human body. For example, lipids are the major component of cell membranes and are assembled into lipid bilayer vesicles, so-called liposomes. Actually, polyethylene glycol modified liposomes exhibit stable circulation in the bloodstream and are effective carriers for anti-cancer reagents [33,34]. The LbL method is suitable for the preparation of capsule carriers because various biopolymers can be incorporated into the LbL multilayers. The preparation method and characteristics of the capsules prepared by the LbL method are described in next section.

I.2.2 Layer-by-layer assembled capsules

LbL multilayers can be formed not only on planar substrates but also on curved substrates, as long as the interaction between the substrates and adsorbing molecules exists. As shown in Fig I.9, by using colloidal particles as substrates for polyelectrolyte

multilayers, and following the dissolution of the particles, hollow polyelectrolyte capsules can be obtained. The wall thickness of the capsules can be controlled by the adsorption times of polyelectrolytes and deposition conditions as well as planar LbL multilayer films. In particular, the size and the shape of prepared capsules are almost the same with that of templates. This means that the diameter of the capsules is easily controlled by the dimensions of templates. Sacrificial templates available for the preparation of polyelectrolyte capsules by LbL method have to fulfill some properties: stability under the LbL adsorption, high solubility under the condition where the multilayer is stable, and easy and complete removal of dissolved substances from the interior of the capsules [35]. The colloidal templates that have been frequently used are summarized in Table I.1. In brief, a variety of polymer particles can be employed as the templates by using appropriate organic solvents for the dissolution. Alternatively, some inorganic particles are also suitable. As a peculiar example, red blood cells, erythrocytes, can be used as biological templates by using a hypochlorite solution as a dissolving medium. In particular, the polyelectrolyte capsules templated on echinocytes, which are spike shape and the unusual morphology of human erythrocytes, were successfully prepared mimicking the original shapes of the templates [36]. For the preparation of capsules by the LbL method, it is not necessary to use sacrificial templates. Polyelectrolyte multilayer capsules that have an encapsulation capability can be prepared by polyelectrolyte coating on the surface of liposomes and hydrogel particles without dissolving themselves [37,38].

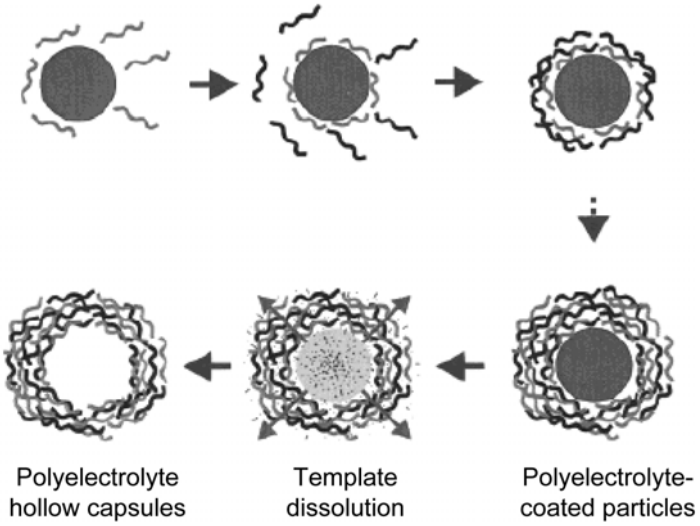

Fig. I.9 Schematic illustration of the preparation procedure of hollow polyelectrolyte multilayer capsules [39].

Interestingly, it was reported that the permeability of prepared capsules is different depending on the sacrificial templates in spite of the same composition and thickness of multilayers [35]. For example, hollow capsules templated on melamine formaldehyde (MF) show much higher permeability than multilayers deposited on planar substrates. Low molecular weight of dye molecules can penetrate the multilayers of capsules but not planar multilayers, which have the separation potential for nanofiltration membrane [40,41]. In contrast, hollow capsules templated on silica prevent the permeation of small dye molecules, rhodamine 6G, which can penetrate the shell of the capsules prepared from MF [35]. This difference is because MF oligomers produced by the dissolution of the templates induce an osmotic swelling pressure inside the capsules. When the resulting oligomers do not permeate through the capsule wall quickly, this mechanical stress further increases and would rupture the capsules [42]. For another example of polymer templates, polystyrene latices, which can be dissolved in tetrahydrofuran, are

swollen during the dissolution procedure [35]. The swelling of the templates induces defects in the capsule wall. In the case of inorganic templates, silica is dissolved by hydrofluoric acid, releasing small ions outside the capsules without the mechanical stress and the swelling. Thus, intact hollow capsules can be obtained. For the same reason, inorganic carbonate crystals can be also used as templates that are dissolved without above problems [35].

Table I.1 Templates used for the preparation of hollow polyelectrolytes capsules [35].

Parameter	Melamine formaldehyde	Polystyrene latex	Polylactic acid	Silica	$CaCO_3$, $MnCO_3$, $CdCO_3$	Erythrocytes
size [µm]	0.3–10	0.1–5	0.2–20	0.03–100	3–8	5.5–7.5
shape	spherical	spherical	spherical	spherical	crystalline; porous	discocytes
monodispersity	excellent	excellent	low	good–excellent	medium	good
commercial availability	+	+	+/–	+	–	+
price	very high	medium	low	low	–	low
problems upon dissolution	mechanical stress; residues	mechanical stress; residues	residues	aggregation	no stress	chemical stress; wall destruction

I.3 Purpose of this study

In this study, the preparation of functional polyelectrolyte capsules by using the LbL method is focused. The substrates used are the following two kinds: hydrogel microspheres and calcium carbonate microparticles. The aims of this study are to introduce advanced functionalities into existing hydrogel microspheres and to prepare novel microcapsules through the following described studies.

Hydrogels show a growing interest as drug carriers due to high loading capacity and stimuli responsive release [43]. LbL-coated microgels with polyelectrolytes would form core-shell type microparticles with multilayers as the shells and will show a function of

the diffusion barrier for encapsulated compounds. In this study, pH-responsive microgels were adopted as substrates. pH-responsive drug release is available in human body, because slightly acidic environments of tumors (pH 6.5–7.2), endosomes (pH 5.0–6.5), and lysosomes (pH 4.5–5.0) can be used as a trigger [44]. As described above, it is considered that polyelectrolyte-coated microgels have a potential use as drug carriers. Nevertheless, little studies have been reported on such core-shell microgels. So far as known, LbL-coated poly(N-isopropylacrylamide) microgels have been only studied by Wong et al. [45]. Thus, this study would be expected to provide basic knowledge about this new pH-responsive microcapsule.

The drawbacks of traditional LbL method are time-consuming process and multicomponent systems that need at least two components. Single-component materials may be favorable in some cases, such as requiring high biocompatibility and high hydrophilicity. To solve above problems, based on the LbL method, a novel preparation method of hollow microspheres was developed by using calcium carbonate as templates.

I.4 Scope of this thesis

This thesis is divided into the following 5 chapters.

Chaper I introduced the background of this study as well as the purpose of this study. A review of the previous works and the scope of thesis are also given.

Chapter II described the preparation of pH-responsive hydrogel microspheres coated with LbL assembly of polyelectrolytes. LbL-coated anionic microgels exhibited different pH-responsive behavior compared with uncoated micogels. The effects of the type of adsorbed polycations, such as the difference of molecular weight and polymer

chain structure (i.e., linear and branched), were investigated.

Chapter III described the novel method for the preparation of cross-linked polymer hollow capsules. This method was developed by modifying the traditional LbL method by using porous calcium carbonate microparticles as a template. In this study, as the first example of this method, single-component hollow microcapsules from native DNA were prepared. The enzymatic degradability and the permeability of the pepared DNA capsules were also examined.

Chapter IV reported that the preparation technique described in chapter III was modified by using biotin-labeled DNA and NeutrAvidin. This method was based on avidin–biotin interaction, and NeutrAvidn act as cross-linker for DNA. The size dependent permeability of resulting DNA capsules was investigated. In addition, the combination of biotin-labeled DNA and NeutrAvidin was applied to LbL assembled multilayers and LbL multilayer capsules in this study.

Chapter V summarized the conclusions of this dissertation.

References

[1] A.F. Thünemann, M. Müller, H. Dautzenberg, J.F. Joanny, H. Löwen, Polyelectrolyte complexes, Adv. Polym. Sci 166 (2004) 113–171.

[2] J.B. Schlenoff, H. Ly, M. Li, Charge and mass balance in polyelectrolyte multilayers, J. Am. Chem. Soc. 120 (1998) 7626–7634.

[3] C.H. Porcel, J.B. Schlenoff, Compact Polyelectrolyte Complexes: "Saloplastic" Candidates for Biomaterials, Biomacromolecules 10 (2009) 2968–2975.

[4] G. Decher, Fuzzy nanoassemblies: Toward layered polymeric multicomposites, Science 277 (1997) 1232–1237.

[5] G. Decher, J.D. Hong, J. Schmitt, Buildup of ultrathin multilayer films by a self-assembly process: III. Consecutively alternating adsorption of anionic and cationic polyelectrolytes on charged surfaces, Thin solid films 210 (1992) 831–835.

[6] P. Bertrand, A. Jonas, A. Laschewsky, R. Legras, Ultrathin polymer coatings by complexation of polyelectrolytes at interfaces: suitable materials, structure and properties, Macromol. Rapid Commun. 21 (2000) 319–348.

[7] P.K.H. Ho, M. Granström, R.H. Friend, N.C. Greenham, Ultrathin self-assembled layers at the ITO interface to control charge injection and electroluminescence efficiency in polymer light-emitting diodes, Adv. Mater. 10 (1998) 769–774.

[8] B. Tieke, F. van Ackern, L. Krasemann, A. Toutianoush, Ultrathin self-assembled polyelectrolyte multilayer membranes, Eur. Phys. J. E 5 (2001) 29–39.

[9] S.T. Dubas, J.B. Schlenoff, Polyelectrolyte multilayers containing a weak polyacid: Construction and deconstruction, Macromolecules 34 (2001) 3736–3740.

[10] G. Ladam, P. Schaad, J.C. Voegel, P. Schaaf, G. Decher, F. Cuisinier, In situ determination of the structural properties of initially deposited polyelectrolyte

multilayers., Langmuir 16 (2000) 1249–1255.

[11] F. Caruso, K. Niikura, D.N. Furlong, Y. Okahata, 1. Ultrathin multilayer polyelectrolyte films on gold: construction and thickness determination, Langmuir 13 (1997) 3422–3426.

[12] M. Onda, K. Ariga, T. Kunitake, Activity and stability of glucose oxidase in molecular films assembled alternately with polyions, J. Biosci. Bioeng. 87 (1999) 69–75.

[13] K. Ren, J. Ji, J. Shen, Tunable DNA release from cross-linked ultrathin DNA/PLL multilayered films, Bioconjugate Chem. 17 (2006) 77–83.

[14] J. Liu, Y. Jin, A. Wu, Z. Li, S. Dong, Fabrication and characterization of DNA/QPVP-Os redox-active multilayer film, Electroanalysis 16 (2004) 1931–1937.

[15] A.B. Artyukhin, O. Bakajin, P. Stroeve, A. Noy, Layer-by-layer electrostatic self-assembly of polyelectrolyte nanoshells on individual carbon nanotube templates, Langmuir 20 (2004) 1442–1448.

[16] P. Podsiadlo, M. Michel, K. Critchley, S. Srivastava, M. Qin, J.W. Lee, E. Verploegen, A.J. Hart, Y. Qi, N.A. Kotov, Diffusional self-organization in exponential layer-by-layer films with micro- and nanoscale periodicity, Angew. Chem. Int. Ed. 48 (2009) 1–6.

[17] L. Wang, Z. Wang, X. Zhang, J. Shen, L. Chi, H. Fuchs, A new approach for the fabrication of an alternating multilayer film of poly(4-vinylpyridine) and poly(acrylic acid) based on hydrogen bonding, Macromol. Rapid Commun. 18 (1997) 509–514.

[18] G.K. Such, J.F. Quinn, A. Quinn, E. Tjipto, F. Caruso, Assembly of ultrathin polymer multilayer films by click chemistry, J. Am. Chem. Soc. 128 (2006) 9318–9319.

[19] Y. Shimazaki, M. Mitsuishi, S. Ito, M. Yamamoto, Preparation and

characterization of the layer-by-layer deposited ultrathin film based on the charge-transfer interaction in organic solvents, Langmuir 14 (1998) 2768–2773.

[20] C. Camacho, J.C. Matías, R. Cao, M. Matos, B. Chico, J. Hernández, M.A. Longo, M.A. Sanromán, R. Villalonga, Hydrogen peroxide biosensor with a supramolecular layer-by-layer design, Langmuir 24 (2008) 7654–7657.

[21] O. Crespo-Biel, B. Dordi, D.N. Reinhoudt, J. Huskens, Supramolecular layer-by-layer assembly: alternating adsorptions of guest- and host-functionalized molecules and particles using multivalent supramolecular interactions, J. Am. Chem. Soc. 127 (2005) 7594–7600.

[22] S.T. Dubas, J.B. Schlenoff, Factors controlling the growth of polyelectrolyte multilayers, Macromolecules 32 (1999) 8153–8160.

[23] J. Meier-Haack, W. Lenk, D. Lehmann, K. Lunkwitz, Pervaporation separation of water/alcohol mixtures using composite membranes based on polyelectrolyte multilayer assemblies, J. Membr. Sci. 184 (2001) 233–243.

[24] S.S. Shiratori, M.F. Rubner, pH-dependent thickness behavior of sequentially adsorbed layers of weak polyelectrolytes, Macromolecules 33 (2000) 4213–4219.

[25] D. Yoo, S.S. Shiratori, M.F. Rubner, Controlling bilayer composition and surface wettability of sequentially adsorbed multilayers of weak polyelectrolytes, Macromolecules 31 (1998) 4309–4318.

[26] J. Papenhuijzen, G.J. Fleer, B.H. Bijsterbosch, Adsorption of polystyrene sulfonate on polyoxymethylene single crystals at high ionic strength, J. Colloid Interface Sci. 104 (1985) 530–539.

[27] M.A. Cohen Stuart, G.J. Fleer, J. Lyklema, W. Norde, J.M.H.M. Scheutjens, Adsorption of ions, polyelectrolytes and proteins, Adv. Colloid Interface Sci. (1991)

477–535.

[28] Z. Tang, Y. Wang, P. Podsiadlo, N.A. Kotov, Biomedical applications of layer-by-layer assembly: from biomimetics to tissue engineering, Adv. Mater. 18 (2006) 3203–3224.

[29] R. Malaisamy, M.L. Bruening, High-flux nanofiltration membranes prepared by adsorption of multilayer polyelectrolyte membranes on polymeric supports, Langmuir 21 (2005) 10587–10592.

[30] T.M. Allen, P.R. Cullis, Drug delivery systems: entering the mainstream, Science 303 (2004) 1818–1822.

[31] L. Yang, P. Alexandridis, Physicochemical aspects of drug delivery and release from polymer-based colloids, Curr. Opin. Colloid Interface Sci. 5 (2000) 132–143.

[32] I.I. Slowing, J.L. Vivero-Escoto, C.W. Wu, V.S.Y. Lin, Mesoporous silica nanoparticles as controlled release drug delivery and gene transfection carriers, Adv. Drug Delivery Rev. 60 (2008) 1278–1288.

[33] A.L. Klibanov, K. Maruyama, V.P. Torchilin, L. Huang, Amphipathic polyethyleneglycols effectively prolong the circulation time of liposomes, FEBS lett. 268 (1990) 235–237.

[34] N.Z. Wu, D. Da, T.L. Rudoll, D. Needham, A.R. Whorton, M.W. Dewhirst, Increased microvascular permeability contributes to preferential accumulation of stealth liposomes in tumor tissue, Cancer Res. 53 (1993) 3765–3770.

[35] C.S. Peyratout, L. Dähne, Tailor-made polyelectrolyte microcapsules: from multilayers to smart containers, Angew. Chem. Int. Ed. 43 (2004) 3762–3783.

[36] E. Donath, S. Moya, B. Neu, G.B. Sukhorukov, R. Georgieva, A. Voigt, H. Bäumler, H, Kiesewetter, H, Möhwald, Hollow polymer shells from biological

templates: fabrication and potential applications, Chem. Eur. J. 8 (2002) 5481–5485.

[37] K. Fujimoto, T. Toyoda, Y. Fukui, Preparation of bionanocapsules by the layer-by-layer deposition of polypeptides onto a liposome, Macromolecules 40 (2007) 5122–5128

[38] B.G. De Geest, C. Déjugnat, E. Verhoeven, G.B. Sukhorukov, A.M. Jonas, J. Plain, J, Demeester, S.C. De Smedt, Layer-by-layer coating of degradable microgels for pulsed drug delivery, J. Controlled Release 116 (2006) 159–169.

[39] E. Donath, G.B. Sukhorukov, F. Caruso, S.A. Davis, H. Möhwald, Novel hollow polymer shells by colloid-templated assembly of polyelectrolytes, Angew. Chem. Int. Ed. 37 (1998) 2202–2205.

[40] W.F. Dong, J.K. Ferri, T. Adalsteinsson, M. Schönhoff, G.B. Sukhorukov, H. Möhwald, Influence of shell structure on stability, integrity, and mesh size of polyelectrolyte capsules: mechanism and strategy for improved preparation, Chem. Mater. 17 (2005) 2603–2611.

[41] S.U. Hong, M.D. Miller, M.L. Bruening, Removal of dyes, sugars, and amino acids from NaCl solutions using multilayer polyelectrolyte nanofiltration membranes, Ind. Eng. Chem. Res. 45 (2006) 6284–6288.

[42] C. Gao, S. Moya, E. Donath, H. Möhwald, Melamine formaldehyde core decomposition as the key step controlling capsule integrity: optimizing the polyelectrolyte capsule fabrication, Macromol. Chem. Phys. 203 (2002) 953–960.

[43] P.F. Kiser, G. Wilson, D. Needham, A synthetic mimic of the secretory granule for drug delivery, Nature 394 (1998) 459–462.

[44] I.K. Park, K. Singha, R.B. Arote, Y.J. Choi, W.J. Kim, C.S. Cho, pH-responsive polymers as gene carriers, Macromol. Rapid Commun. 31 (2010) 1122–1133.

[45] J.E. Wong, W. Richtering, Surface modification of thermoresponsive microgels via layer-by-layer assembly of polyelectrolyte multilayers, Prog. Colloid Polym. Sci. 133 (2006) 45–51.

Chapter II

pH-responsive Behavior of Hydrogel Microspheres Altered by Layer-by-layer Assembly of Polyelectrolytes

II.1 Introduction

The layer-by-layer (LbL) method is an attractive technique for the fabrication of multilayer thin films with tailored structures and composition [1]. LbL films are typically formed by the consecutive adsorption of oppositely charged polyelectrolytes (i.e., polycations and polyanions) on substrates through electrostatic interactions. The LbL method has been used to deposit multilayers on various planar [2,3] and spherical substrates [4,5]. In particular, colloidal particles have been used mostly as a sacrificial template to prepare hollow microcapsules [6]. The multilayer thicknesses, dimensions, and functionalities of the LbL microcapsules can be controlled by the total number of layers deposited [7,8], the diameter of the template particles [9], and the incorporated material in the multilayer [8,10,11], respectively. Because of their simplicity and flexibility, LbL capsules are promising for a wide variety of applications, including drug delivery vehicles, microreactors, and sensors [4,12]. The LbL assembly is applicable to polymer hydrogel substrates, such as poly(*N*-isopropylacrylamide) (PNIPAM) [13,14], alginate [15,16], dextran [17], and poly(vinyl alcohol) [18] hydrogels. Alginate microgels covered with polyelectrolyte multilayers possessed variable membrane permeability and immunoisolation capability that are required for encapsulated pancreatic islet transplantation [15]. Polyelectrolyte-coated dextran microgels, which can rupture without any external stimulus, were designed for applications in pulsed drug

release systems [17].

In the case of substrates with porous structures (e.g., mesoporous silica spheres [19], calcium carbonate microparticles [20], and dextran microgels [17]), as well as being deposited on the surfaces, polyelectrolytes diffuse into the pores and are adsorbed in the pores. Wong and Richtering reported that PNIPAM microgels with a soft and porous structure exhibited thermal sensitivity variations when they adsorbed polyelectrolytes; the variations depended on the number of deposition cycles [13]. Their study indicates that, in the LbL method, apart from functioning as substrates, porous hydrogels also modify their behavior depending on the adsorbed polyelectrolytes. An understanding of the influence of the adsorbed polyelectrolytes in various types of stimuli-responsive hydrogels would be important in the design and development of new functional composite polyelectrolyte-gel microcapsules.

In this study, we prepared three kinds of LbL assemblies by using an anionic microgel as the core material to verify changes in the pH sensitivity due to the polyelectrolyte-gel interaction and to examine the influence of the different types of polycations deposited on the microgel.

II.2 Experimental section

II.2.1 Materials

Poly(allylamine hydrochloride) (PAH, catalog no. 283223), poly(ethyleneimine) (PEI, branched, catalog no. 181978), chitosan (CHIT, catalog no. 419419), and poly(styrene sulfonate) (PSS, Mw ≈ 70 000) were purchased from Sigma-Aldrich (St. Louis, MO). Linear PEI (catalog no. 24765) was purchased from Polysciences, Inc. (Warrington, PA). Dextran sulfate (DEXS, average Mr ≈ 500 000), methacrylic acid (MAA)

N,*N'*-methylenebisacrylamide (MBAA), and 2,2'-azobisisobutyronitrile (AIBN) were purchased from Wako Pure Chemical Industries (Osaka, Japan). *p*-Nitrophenyl acrylate (NPA) was purchased from Monomer-Polymer and Dajac Labs (Feasterville, PA). *p*-Nitrophenyl methacrylate (NPMA) was synthesized from *p*-nitrophenol and methacryloyl chloride as described by Kiser et al. [21]. MAA was distilled under reduced pressure before use. NPA and NPMA were purified by recrystallization from ethyl acetate/hexane (1:2 v/v).

II.2.2 Molecular weight determination of polycations

The molecular weights of used polycations, PAH, branched PEI (bPEI), linear PEI (lPEI), and CHIT, were determined by size exclusion chromatography (SEC) using a Shodex OHpak SB-805HQ column (Showa Denko, Tokyo, Japan) and a refractive index detector (RID-10A; Shimadzu Corp., Kyoto, Japan). As eluents, the following solutions were prepared: Eluent A, 0.5 M acetic acid (AcOH) and 0.1 M sodium nitrate ($NaNO_3$); Eluent B, 0.5 M AcOH and 0.5 M sodium acetate (AcONa); and Eluent C, 0.5 M AcONa buffer (pH 3.7). The types of eluents used for each measurement are summerized in Table II.1. Number and weight average molecular weights were calculated from calibration curves obtained from poly(ethylene glycol)/poly(ethylene oxide) standards.

II.2.3 Preparation of microgels

Hydrogel microspheres (with a mean diameter of 9.4 μm at pH 6.5) were synthesized by precipitation polymerization, which was developed by Kashiwabara et al. [22] and modified by Kiser et al. [21]. In brief, an alcohol mixture (20 ml of ethanol and 8 ml of methanol) containing monomers (11 mmol of NPA, 11 mmol of MAA, and 2.5 mmol of MBAA) was degassed by bubbling N_2. The reaction medium was then heated to 60 °C,

and this was followed by the addition of an initiator solution (1.5 g of AIBN in 12 ml of acetone) to initiate the polymerization. The resulting microparticles were dispersed in 1 M NaOH to obtain anionic microgels by the hydrolysis of *p*-nitrophenyl esters.

Table II.1. Average molecular weights of polycations measured by SEC

Polycation	*M* w	*M* n	Eluent[a]
PAH	91 000	20 000	A
bPEI	200 000	3 400	A
lPEI	20 000	5 200	B
CHIT	950 000	140 000	C

[a] Eluent A: 0.5 M AcOH + 0.1 M $NaNO_3$, B: 0.5 M AcOH + 0.5 M AcONa, C: 0.5 M AcONa buffer (pH 3.7)

II.2.4 Polyelectrolyte LbL method

We adopted three kinds of polyelectrolyte pairs for adsorption onto the microgels for the LbL method: PAH–PSS, bPEI–PSS, and CHIT–DEXS. The assemblies were prepared as follows. An aqueous dispersion of microgels (approximately 0.1 wt% in deionized water, 100 μl) was mixed with the polyelectrolyte solution (10 mg/ml in deionized water, 100 μl) and 50 mM imidazole-HCl buffer (pH 6.5, adjusted with NaCl to ionic strength I = 0.63 M, 800 μl). The mixture was incubated for 20 min at room temperature with gentle shaking. After each adsorption, the microgels were washed three times by centrifugation with deionized water to remove excess polyelectrolyte. This procedure was repeated for the oppositely charged polyelectrolyte. For the case of CHIT adsorption, a saturated CHIT solution in 0.1 M AcONa buffer (pH 5.0, adjusted with NaCl to I = 0.2 M, 900 μl) was used as the polyelectrolyte solution, and 0.1 M AcONa buffer (pH 5.0) was used as the washing solution. In all the cases, six consecutive adsorption steps were carried out. The architectures of the resultant

assemblies are represented as follows: $(PAH/PSS)_3$, $(bPEI/PSS)_3$, and $(CHIT/DEXS)_3$.

II.2.5 Characterization

The electrophoretic mobility of LbL-coated microgels in 10 mM NaCl solution was measured using a spectrophotometer (ELS-6000; Otsuka Electronics Co., Ltd., Osaka, Japan). In this measurement, small microgels (with a mean diameter of 1.3 μm and a monomer composition of NPA/MAA/MBAA in the ratio 11:11:2.5 mmol) were used as an alternative to the larger microgels to avoid the effects of the rapid sedimentation of particles. The ζ-potential was calculated from the electrophoretic mobility using the Smoluchowski relation. Optical images of microgels were obtained using an MRC-1024 confocal microscope (Bio-Rad, Hercules, CA). To visualize the location of polyelectrolytes adsorbed on the microgels, we added tetramethylrhodamine isothiocyanate (TRITC)-labeled polycations to the polycation solution in the adsorption step. The influence of the pH on the microgel size was evaluated by observing the change in the microgel mean diameter within 10 min of the immersion of the microgel in solutions with different pH values: 50 mM solutions of glycine-HCl (pH 2–3), sodium phosphate (4–5.5), imidazole-HCl (6.5–7.5), Tris-HCl (8–8.5), and glycine-NaOH (9–12) buffer. The ionic strength of each buffer solution was adjusted to 0.06 M with NaCl. The surface morphology of polyelectrolyte-gel complexes on microgels was observed by field-emission scanning electron microscopy (FE-SEM) (JSM-7500F; JEOL Ltd., Tokyo, Japan) operating at an accelerating voltage of 5 kV. The samples were prepared by placing a drop of the microgel dispersion onto a freshly cleaved mica surface and then lyophilizing.

II.3 Results and Discussion

The LbL deposition of the polyelectrolytes onto the microgels was monitored by electrophoretic mobility measurements, as shown in Fig. II.1. The ζ-potential of the uncoated microgels was −26 mV and alternated between +50 and −40 mV during the adsorption cycle. Similar ζ-potential changes were observed during the bPEI/PSS and CHIT/DEXS adsorptions. However, ζ-potential measurements do not provide apparent evidence for multilayer growth because they cannot distinguish between consecutive adsorptions on surfaces and the desorption of deposited polyelectrolytes [7,14]. Therefore, the third deposited layer of polycations was labeled with TRITC and observed by confocal microscopy (Fig. II.2, right column). Homogeneous coverage on the microgels was confirmed; it indicates a successful multilayer buildup up to the third deposited layer.

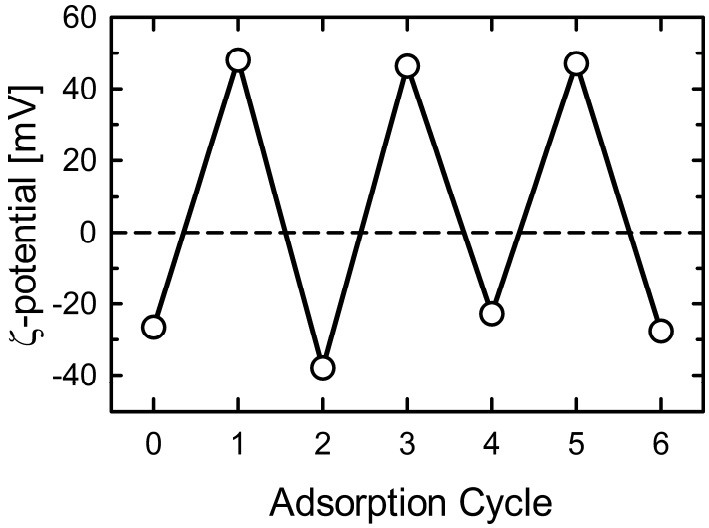

Figure II.1. ζ-potential of $(PAH/PSS)_3$ microgels after each adsorption cycle. The measurements were performed in 10 mM NaCl solution.

Typical optical images of the LbL-coated microgels are shown in Fig. II.2. $(PAH/PSS)_3$ microgels had two distinct areas: an approximately 1.5-μm-thick outer layer and a core (Fig. II.2A, left). This outer layer had already formed when the first adsorption step involving the adsorption of PAH ended, and the area penetrated by TRITC-labeled PAH (Fig. II.2A, middle) agreed with the location of this layer. Therefore, PAH chains that penetrated the microgel formed a complex with the polymer chains of the hydrogel. The area penetrated by the PAH was condensed and converted into a polyelectrolyte-gel "complex shell" owing to the compensation of the electrostatic repulsion between the negative charges in the hydrogel. From the image of $(bPEI/PSS)_3$ microgels (Fig. II.2B, middle), we confirmed that the bPEI chains used in the first adsorption step penetrated to the center of the microgels. As shown in Fig. II.2B (right), the bPEI chains used in the third adsorption step led to layer formation on the microgel. The area penetrated by the polycations in the $(bPEI/PSS)_3$ microgels was larger than that in the $(PAH/PSS)_3$ microgels. The average diameter of the former was slightly larger than that of the latter (7.0 ± 0.9 μm vs. 6.0 ± 0.6 μm). This is because the $(bPEI/PSS)_3$ microgels did not shrink to such an extent that the complex shell as the $(PAH/PSS)_3$ microgels formed. The mechanism of the microgel shrinkage is as follows: an ionic hydrogel which interacted with oppositely charged polyelectrolytes releases small counterions to a surrounding aqueous medium and result in a dehydration (a volume decrease) because of the decrease of the osmotic pressure inside the hydrogel. The volume of the hydrogel depends on the amount of mobile counterions confined in the hydrogel. Rogacheva et al. reported that polyelectrolyte gels and oppositely charged linear polyelectrolytes form a stoichiometric interpolyelectrolyte complex in neutral pH solutions [23]. Thus, in our experiments, we considered that the penetrated PAH chain

(linear structure) compensated a large portion of the negative charges inside the microgel and caused the microgel to shrink. While in the case of branched PEI, low shrinkage of the microgel would be due to non-stoichiometric complex formation.

$(CHIT/DEXS)_3$ microgels maintained their original size (9.8 ± 0.9 μm at pH 6.5). It can be observed from Fig. II.2C that CHIT chains were deposited almost at the edge of the microgel surface. Thus, shrinkage of the microgels was not observed after the CHIT/DEXS adsorption process.

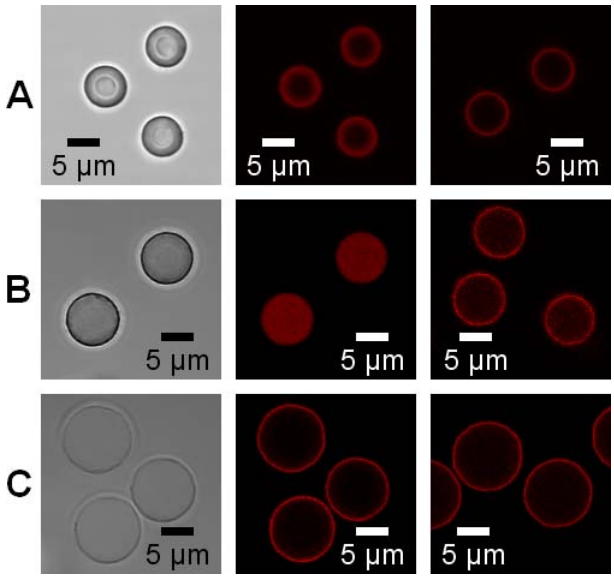

Figure II.2. Transmission (left) and confocal (middle and right) microscopy images of LbL-coated microgels: (A) $(PAH/PSS)_3$, (B) $(bPEI/PSS)_3$, and (C) $(CHIT/DEXS)_3$. The first (middle) and third (right) deposited layer of the polycations were fluorescently labeled with TRITC. The microgels were suspended in a buffer solution (pH 6.5).

The FE-SEM images of uncoated and coated microgels are shown in Fig. II.3. For all kinds of microgels, significant shrinkage was observed due to drying during the sample

preparation. The uncoated microgel had a smoother surface compared with the coated microgels. The coated microgels prepared with PAH, bPEI, and CHIT adsorption exhibited a granular, a "brain-like", and a highly wrinkled surface, respectively (Fig. II.3B, C, and D). The wrinkled surface of the CHIT-coated microgel, in partcular, was probably induced by a difference in the degree of shrinkage between the microgel core and a surrounding thin complex layer. Although a porous structure of the uncoated microgels could not be observed as shown in Fig. II.3A because of the shrinkage, the microgel would have nano-sized pores that allow the diffusion of polyelectrolytes into the cross-linked polymer network, considering the results of confocal microscopy.

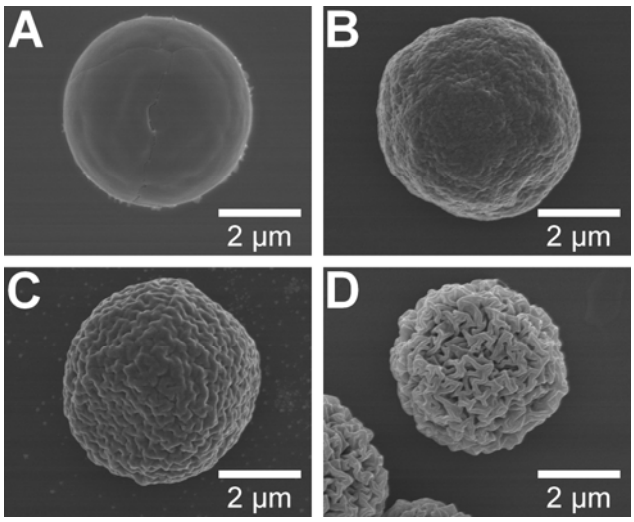

Figure II.3. FE-SEM images of an uncoated microgel and coated microgels obtained after the first polycation adsorption step: (A) uncoated, (B) PAH, (C) bPEI, and (D) CHIT.

Figure II.4 shows the changes in the diameter of the uncoated and the LbL-coated microgels as a function of the pH. The pH-response of the uncoated PMA-co-AA

microgels (control) is consistent with previously reported data [21]. The $(PAH/PSS)_3$ microgels maintained a diameter of 6.0 ± 0.6 μm in the pH 4 to 10 range and swelled outside this pH range (Fig. II.4A). This swelling can be attributed to charge imbalance in the complex shell. In other words, the carboxyl groups of the microgel are protonated at low pH, whereas the amino groups of PAH become deprotonated at high pH. The large amount of excess charges in the complex shell attract counterions from the bulk solution, and therefore, the increased osmotic pressure inside the multilayer results in the swelling of the $(PAH/PSS)_3$ microgels. Such pH-responsive swelling behavior is similar to that of PAH–poly(methacrylic acid) hollow LbL capsules [24]. Figure II.4B shows the remarkable swelling of $(bPEI/PSS)_3$ microgels at low and high pH. The most condensed state was observed at around pH 8.5. This indicates that at pH 8.5, the amount of positive charge provided by the penetrated bPEI chains (Fig. II.2B, middle) is almost equal to that of the negative charge provided by the carboxyl groups inside the microgel. Consequently, the net electrostatic charge inside the $(bPEI/PSS)_3$ microgel becomes positive and negative at pH less than 8 and greater than 9, respectively. In other words, $(bPEI/PSS)_3$ microgel appeared to behave like an amphoteric microgel [22]. As shown in Fig. II.4C, the $(CHIT/DEXS)_3$ microgels exhibited the same pH-response as did the uncoated gels at pH greater than 4. However, in the most condensed state, the average diameter of the former was larger than that of the latter. The low shrinkage at low pH is probably due to the physical restriction imposed by the surrounding polyelectrolyte multilayer.

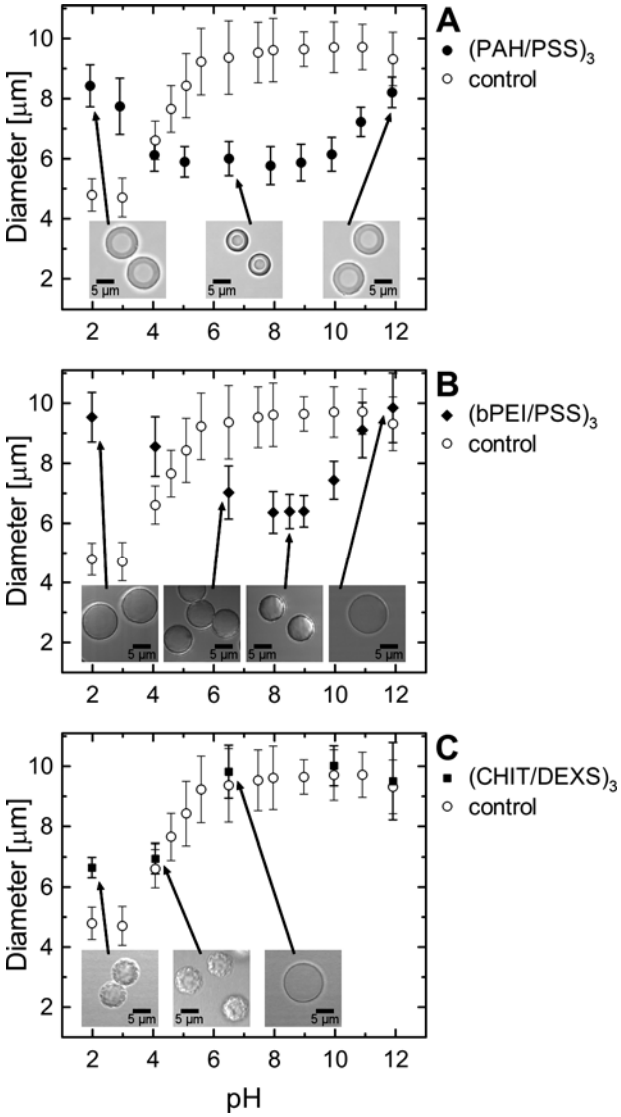

Figure II.4. Effect of pH on LbL-coated microgel diameter: (A) $(PAH/PSS)_3$, (B) $(bPEI/PSS)_3$, and (C) $(CHIT/DEXS)_3$. Insets show transmission microscopy images of microgels. Values are means ± SD of 50 individual

These differences in the pH-responses of the LbL-coated microgels could be due to the differences in the molecular weights and polymer chain structures of the polycations.

Table II.1 shows the SEC results of used polycations. The molecular weight of CHIT was much higher than that of the others. High molecular weight molecules whose hydrodynamic diameters are larger than the mesh sizes of the microgel network cannot penetrate the microgel. Thus, CHIT chains did not penetrate the microgel and the pH-response of the $(CHIT/DEXS)_3$ microgel was similar to that of the control microgel. As mentioned previously, the penetrated PAH chain, which has a linear structure that penetrated the microgel network compensates a large portion of the negative charges inside the microgel and causes the microgel to shrink. In contrast, the bPEI chain tends to overcompensate the charge of the microgel because of the existence of charged PEI segments, which do not interact with the carboxyl groups inside the microgel. This excess positive charge produces electrostatic repulsion that prevents the collapse of the network. To confirm this, we used an lPEI as well as the bPEI and carried out only the first PEI-adsorption step. Figure II.5 shows the size differences of two types of PEI-adsorbed microgels after the uncoated microgels were incubated in each of the PEI solutions. Both types of PEI chains penetrated to the center of the microgels, presumably owing to the presence of lower molecular weight components than those of PAH (Table II.1). When lPEI was used instead of bPEI, the higher shrinkage of the microgel was confirmed because of low excess charge.

When comparing Fig. II.2B with Fig. II.5A, one observes that the diameter of the $(bPEI/PSS)_3$ microgels was smaller than that of the microgels obtained after the first bPEI-adsorption step. This suggests the possibility of the penetration of PSS chains into the microgels. However, as shown in Fig. II.4B, the most condensed state of the $(bPEI/PSS)_3$ microgels was observed at around pH 8.5. This indicates that PSS chains could not compensate a large portion of the positive charges inside the microgel. In the

case of the $(PAH/PSS)_3$ microgels, PSS chains cannot penetrate to the core area (inside) of the micorgel probably owing to the electrostatic repulsion between the PSS chains and the core area. Therefore, we consider that the PSS penetration does not affect the pH-response of the microgels critically.

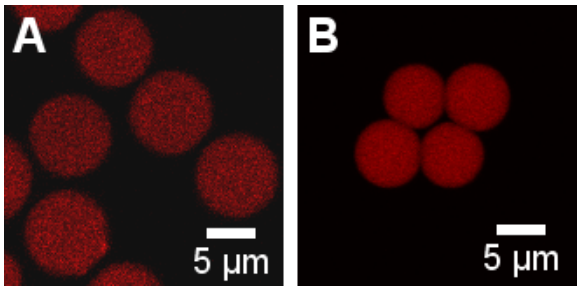

Figure II.5. Confocal microscopy images of the microgels after the adsorption treatment with TRITC-labeled (A) bPEI and (B) lPEI. The microgels were observed in a pH 6.5 buffer solution.

Finally, we observed $(CHIT/DEXS)_3$ microgels in solutions with varying pH with confocal microscopy. The result is shown in Fig. II.6. At low pH, CHIT/DEXS multilayer shrunk together with the microgel core and became wrinkled. After the pH was changed from 2.0 to 6.5, the microgel became swollen within a couple of minutes, and the multilayer remained on the microgel. This result suggests that the LbL-coated microgels have a reversible pH-response, and it shows the mechanical stability of the multilayer.

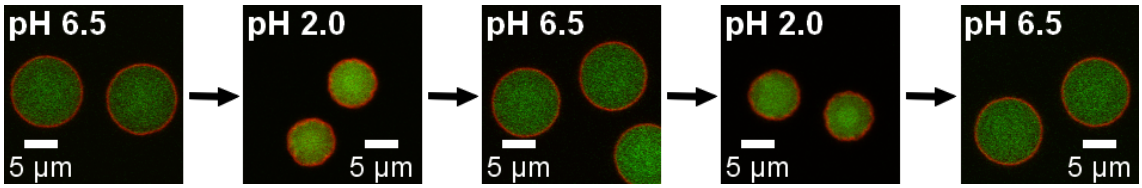

Figure II.6. Confocal microscopy images of $(CHIT/DEXS)_3$ microgels in pH varying between 2.0 and 6.5. The fifth deposited layer was labeled with TRITC. The carboxyl groups of the microgel were conjugated with rhodamine

II.4. Conclusion

We used the layer-by-layer method with an anionic microgel as the substrate and observed the pH-responsive behavior of the microgel. In this study, three types of LbL-coated microgels were prepared. Core-shell microgels with a thick "complex shell," quasi-amphoteric microgels, and anionic microgels covered with a polyelectrolyte multilayer were prepared by using $(PAH/PSS)_3$, $(bPEI/PSS)_3$, and $(CHIT/DEXS)_3$, respectively. This indicates that polycation characteristics such as the molecular weight and polymer chain structure (i.e., linear and branched) strongly influenced the properties of these LbL-coated microgels. In particular, the "complex shell" is expected to be capable of sustained release and retention of entrapped low molecular weight compounds, such as chemicals and drugs. Further investigation of the permeation properties of the shells and multilayers on these LbL-coated microgels is in progress.

References

[1] G. Decher, Fuzzy nanoassemblies: toward layered polymeric multicomposites, Science, 277 (1997) 1232–1237.

[2] P. Bertrand, A. Jonas, A. Laschewsky, R. Legras, Ultrathin polymer coatings by complexation of polyelectrolytes at interfaces: suitable materials, structure and properties, Macromol. Rapid Commun., 21 (2000) 319–348.

[3] B. Tieke, F. van Ackern, L. Krasemann, A. Toutianoush, Ultrathin self-assembled polyelectrolyte multilayer membranes, Eur. Phys. J. E, 5 (2001) 29–39.

[4] C.S. Peyratout, L. Dähne, Tailor-made polyelectrolyte microcapsules: from multilayers to smart containers, Angew. Chem. Int. Ed., 43 (2004) 3762–3783.

[5] L.M.C. Sagis, R. de Ruiter, F.J.R. Miranda, J. de Ruiter, K. Schroën, A.C. van Aelst, H. Kieft, R. Boom, E. van der Linden, Polymer microcapsules with a fiber-reinforced nanocomposite shell, Langmuir 24 (2008) 1608–1612.

[6] C. Gao, S. Moya, E. Donath, H. Möhwald, Melamine formaldehyde core decomposition as the key step controlling capsule integrity: optimizing the polyelectrolyte capsule fabrication, Macromol. Chem. Phys., 203 (2002) 953-960.

[7] G.B. Sukhorukov, E. Donath, H. Lichtenfeld, E. Knippel, M. Knippel, A. Budde, H. Möhwald, Layer-by-layer self assembly of polyelectrolytes on colloidal particles, Colloids Surf. A, 137 (1998) 253–266.

[8] K. Glinel, G.B. Sukhorukov, H. Möhwald, V. Khrenov, K. Tauer, Thermosensitive hollow capsules based on thermoresponsive polyelectrolytes, Macromol. Chem. Phys., 204 (2003) 1784–1790.

[9] H. Zhu, E.W. Stein, Z. Lu, Y.M. Lvov, M.J. McShane, Synthesis of size-controlled monodisperse manganese carbonate microparticles as templates for uniform

polyelectrolyte microcapsule formation, Chem. Mater., 17 (2005) 2323–2328.

[10] Y. Ma, W.F. Dong, M.A. Hempenius, H. Möhwald, G.J. Vancso, Redox-controlled molecular permeability of composite-wall microcapsules, Nat. Mater., 5 (2006) 724–729.

[11] A.S. Angelatos, B. Radt, F. Caruso, Light-responsive polyelectrolyte/gold nanoparticle microcapsules, J. Phys. Chem. B, 109 (2005) 3071–3076.

[12] A.P.R. Johnston, C. Cortez, A.S. Angelatos, F. Caruso, Layer-by-layer engineered capsules and their applications, Curr. Opin. Colloid Interface Sci., 11 (2006) 203–209.

[13] J.E. Wong, W. Richtering, Surface modification of thermoresponsive microgels via layer-by-layer assembly of polyelectrolyte multilayers, Prog. Colloid Polym. Sci., 133 (2006) 45–51.

[14] J.E. Wong, C.B. Müller, A. Laschewsky, W. Richtering, Direct evidence of layer-by-layer assembly of polyelectrolyte multilayers on soft and porous temperature-sensitive PNiPAM microgel using fluorescence correlation spectroscopy, J. Phys. Chem. B, 111 (2007) 8527–8531.

[15] S. Schneider, P.J. Feilen, V. Slotty, D. Kampfner, S. Preuss, S. Berger, J. Beyer, R. Pommersheim, Multilayer capsules: a promising microencapsulation system for transplantation of pancreatic islets, Biomaterials, 22 (2001) 1961–1970.

[16] H. Zhu, R. Srivastava, M.J. McShane, Spontaneous loading of positively charged macromolecules into alginate-templated polyelectrolyte multilayer microcapsules, Biomacromolecules, 6 (2005) 2221–2228.

[17] B.G. De Geest, C. Déjugnat, E. Verhoeven, G.B. Sukhorukov, A.M. Jonas, J. Plain, J. Demeester, S.C. De Smedt, Layer-by-layer coating of degradable microgels for pulsed drug delivery, J. Controlled Release, 116 (2006) 159–169.

[18] T. Serizawa, H. Sakaguchi, M. Matsusaki, M. Akashi, Polyelectrolyte multilayers prepared on hydrogel surfaces, J. Polym. Sci. Part A, 43 (2005) 1062–1067.

[19] Y. Wang, A. Yu, F. Caruso, Nanoporous polyelectrolyte spheres prepared by sequentially coating sacrificial mesoporous silica spheres, Angew. Chem. Int. Ed., 44 (2005) 2888–2892.

[20] D.V. Volodkin, A.I. Petrov, M. Prevot, G.B. Sukhorukov, Matrix polyelectrolyte microcapsules: new system for macromolecule encapsulation, Langmuir, 20 (2004) 3398–3406.

[21] P.F. Kiser, G. Wilson, D. Needham, Lipid-coated microgels for the triggered release of doxorubicin, J. Controlled Release, 68 (2000) 9–22.

[22] M. Kashiwabara, K. Fujimoto, H. Kawaguchi, Preparation of monodisperse, reactive hydrogel microspheres and their amphoterization, Colloid Polym. Sci., 273 (1995) 339–345.

[23] V.B. Rogacheva, V.A. Prevysh, A.B. Zezin, V.A. Kabanov, Interpolymer reactions between network and linear polyelectrolytes, Polym. Sci. U.S.S.R., 30 (1988) 2262-2270.

[24] T. Mauser, C. Déjugnat, G.B. Sukhorukov, Reversible pH-dependent properties of multilayer microcapsules made of weak polyelectrolytes, Macromol. Rapid Commun., 25 (2004) 1781–1785.

Chapter III

Cross-linked DNA capsules templated on porous calcium carbonate microparticles

III.1 Introduction

Polymer capsules have attracted increasing interest because of their potential applications in drug delivery, sensing, catalyst, and encapsulation [1–4]. They can be prepared by a variety of physical and chemical techniques, such as self-assembly, templating, phase separation, and emulsion polymerization [3,5,6]. Of these methods, the layer-by-layer (LbL) method is effective in building up polyelectrolyte multilayers onto solid substrates with controlled thickness and composition [7]. In the past decade, the LbL method has been intensively studied, and various polymer capsules with versatile functions have been obtained with different polymers [8,9]. Stimuli-responsive [10–13], degradable [14–16], and low-fouling capsules [16] are examples of such functional capsules. However, a conventional LbL method requires at least two components to stabilize the assemblies via intermolecular interactions. These multicomponent capsules may be inadequate for certain applications requiring the properties of each individual component rather than its complex.

Several modified LbL methods have been developed to construct single-component capsules. Chitosan, poly(methacrylic acid), and poly(*N*-vinylpyrrolidone) capsules were prepared by selective cross-linking of one component followed by removal of other components from an LbL assembly [16–18]. Poly(allylamine hydrochloride) capsules were prepared by a covalent LbL assembly method utilizing glutaraldehyde [19].

Cross-linked protein microcapsules prepared by this covalent LbL assembly method retained the biocatalytic activity of constituent proteins without denaturation [20,21]. Another covalent LbL assembly method based on click chemistry, which needs azide- and alkyne-functionalized polymers, was recently reported [22]. One drawback common to the above LbL methods is that a time-consuming sequential adsorption process is needed to reach a given shell thickness.

More recently, Wang et al. developed a new method for the preparation of single-component polyelectrolyte capsules by using mesoporous shell silica particles as sacrificial templates [23]. The significant advantage of this method is that monodispersed capsules with considerably thicker shells, when compared with the thickness of LbL assemblies, can be obtained with only a single adsorption step. However, the use of toxic hydrofluoric acid, which is necessary to dissolve the silica, is unavoidable.

Herein, we present an alternative method for the preparation of single-component capsules by using porous calcium carbonate ($CaCO_3$) microparticles as templates. $CaCO_3$ can be dissolved under mild conditions with ethylenediaminetetraacetic acid (EDTA). In addition, the porous $CaCO_3$ microparticles have the ability to adsorb diverse macromolecules, such as polyelectrolytes, proteins, and polysaccharides [24–26]. As the first example of this method, we employed DNA as a constituent of the capsule shell. DNA as a biomaterial has received attention for biological and biomedical applications, owing to its biocompatibility, biodegradability, sequence-specific hybridization, and molecular recognition [27–29]. To our knowledge, this is the first preparation of micro-sized single-component hollow capsules from native DNA, even though those from synthetic DNA have been reported by Johnston et al. [30,31].

Scheme III.1 shows the typical preparation procedure of the cross-linked DNA capsules, involving the following steps: (1) DNA adsorption onto and penetration into porous $CaCO_3$ microparticles (termed as the first coating), (2) covalent cross-linking of adsorbed DNA with ethylene glycol diglycidyl ether (EGDE), (3) additional adsorption of DNA onto the $CaCO_3$ microparticles (termed as the additional coating), and (4) the removal of $CaCO_3$ microparticles with EDTA. As an additional advantage, this preparation technique does not require any organic solvent, including in the preparation of templates. In this study, we established a procedure to prepare DNA capsules by the above method, and investigated the enzymatic degradability and the permeability of the prepared DNA capsules.

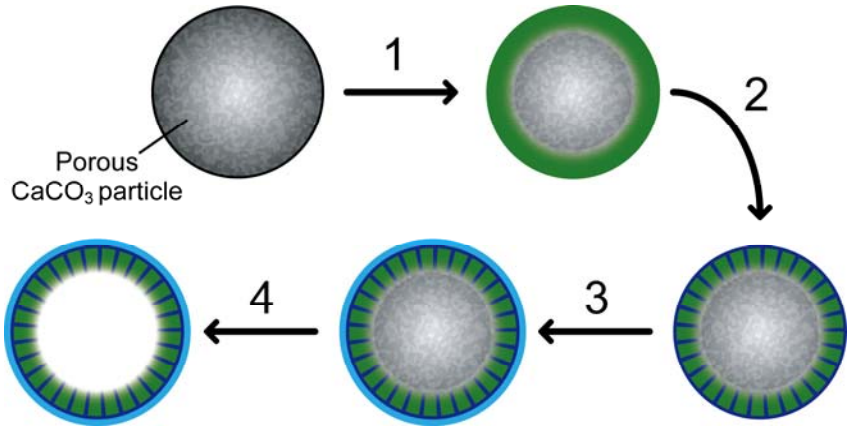

Scheme III.1. Schematic illustration of the preparation process of the cross-linked DNA capsules by using porous $CaCO_3$ microparticles as templates: the first DNA coating (step 1), cross-linking with EGDE (step 2), the additional DNA coating (step 3), and dissolution of CaCO3 microparticles with EDTA (step 4).

III.2 Experimental section

III.2.1 Materials

The sources of chemicals used were as follows: single-stranded salmon testes DNA (10 mg/ml, catalog no. D7656, lot no. 038K62571) was from Sigma-Aldrich (St. Louis, MO); ethylene glycol diglycidyl ether (EGDE, epoxide equivalent weight of 110–120 g/eq), *N*,*N*,*N'*,*N'*-tetramethylethylenediamine (TEMED), sodium carbonate (Na_2CO_3), calcium chloride dihydrate ($CaCl_2 \cdot 2H_2O$), and magnesium chloride hexahydrate ($MgCl_2 \cdot 6H_2O$) were from Wako Pure Chemical Industries (Osaka, Japan); ethylenediaminetetraacetic acid disodium salt dihydrate ($EDTA \cdot 2Na \cdot 2H_2O$) was from Sigma-Aldrich; deoxyribonuclease I from bovine pancreas (DNase I) was from Wako Pure Chemical Industries; and fluorescein isothiocyanate-dextran (FITC-dextran, *M*r ≈ 2,000,000), FITC-dextran (*M*r ≈ 250,000), and tetramethylrhodamine isothiocyanate-dextran (TRITC-dextran, *M*r ≈ 4,400) were from Sigma-Aldrich. The DNA solution was heated at 100 °C for 10 min for denaturation and cooled immediately in an ice–water bath for 10 min before use. All of the other reagents were used as received.

The water used in all experiments was prepared with a Milli-Q® Integral water purification system (Millipore, Bedford, MA) and had a resistivity of 18.2 MΩ·cm. The pH of solutions was adjusted with NaOH if necessary.

III.2.2 Preparation of porous $CaCO_3$ microparticles

$CaCO_3$ microparticles were prepared according to Volodkin et al. [32]. In brief, 0.33 M Na_2CO_3 aqueous solution (80 ml) was rapidly poured into an equal volume of 0.33 M $CaCl_2$ solution under vigorous stirring and then mixed for 30 s. The resultant $CaCO_3$ microparticles were washed twice with water by centrifugation at 500*g* for 1 min,

further washed and collected by filtration, and then dried under vacuum at room temperature.

III.2.3 Preparation of cross-linked DNA capsules

III.2.3.1 DNA capsules cross-linked with TEMED as an additive

For the adsorption of DNA, an aqueous suspension of $CaCO_3$ microparticles (10% solids, 100 μl) was mixed with a DNA solution (10 mg/ml, 200 μl) and 10 mM HEPES buffer (pH 7.0, 700 μl). The mixture was incubated for 20 min at room temperature with gentle shaking. To remove excess DNA, the $CaCO_3$ microparticles were washed four times with water by centrifugation at 250*g* for 3 min. The adsorbed DNA strands were cross-linked as follows. DNA-adsorbed $CaCO_3$ microparticles (10% solids, 100 μl) were added to 4.9 ml of an aqueous solution containing 300 mM EGDE and 100 mM TEMED, and gently shaken for 24 h at room temperature. After the cross-linking and the centrifugation-washing steps with water, DNA was adsorbed once again onto the $CaCO_3$ microparticles in the same manner as described above. In the case of preparing more cross-linked DNA capsules, this cross-linking and the additional DNA adsorption step were repeated once. To obtain DNA capsules, the $CaCO_3$ microparticles were exposed to a 0.05 M EDTA solution (pH 7.0) for 10 min for the removal of the $CaCO_3$ templates. The DNA capsules were washed with 10 mM HEPES buffer (pH 7.0) and subsequently with water by using centrifugal filter units with a 0.2-μm pore size (Vivaspin; Sartorius, Göttingen, Germany) at 50*g*. The DNA capsules obtained after the second coating step and after the third coating step are designated as DNA_2(TEMED) and DNA_3(TEMED) capsules, respectively.

III.2.3.2 DNA capsules cross-linked with NaOH as an additive

For the cross-linking of DNA strands, DNA-adsorbed $CaCO_3$ microparticles (10%

solids, 100 μl) were added to 4.9 ml of an aqueous solution containing 300 mM EGDE and 10 mM NaOH (instead of TEMED), and gently shaken for 24 h at room temperature. After the cross-linking, the $CaCO_3$ templates were removed with the EDTA solution, and then the DNA capsules were washed with water, as described above. The DNA capsules prepared in this way are denoted as DNA_1(NaOH) capsules.

III.2.4 Characterization of $CaCO_3$ microparticles

Nitrogen adsorption–desorption measurement was carried out with a BELSORP-mini (BEL Japan, Inc., Osaka, Japan). Before the measurement, the sample was dried for 3 h at 200 °C under a stream of nitrogen. The surface area and the pore size distribution were calculated by the Brunauer–Emmett–Teller (BET) and the Barrett–Joyner–Halenda (BJH) methods, respectively. The surface morphology of the DNA-adsorbed $CaCO_3$ microparticles was observed by field-emission scanning electron microscopy (FE-SEM) (JSM-7500F; JEOL Ltd., Tokyo, Japan) operating at an accelerating voltage of 4 kV. The samples were prepared by placing a drop of the suspension of the $CaCO_3$ microparticles onto a freshly cleaved mica surface and then lyophilizing. The electrophoretic mobility of the DNA-adsorbed $CaCO_3$ microparticles was measured with a zeta potential analyzer (ELSZ-2; Otsuka Electronics Co., Ltd., Osaka, Japan). In this measurement, the suspensions of the $CaCO_3$ microparticles (0.1% solids in 10 mM HEPES buffer, pH 7.0) were analyzed at 25 °C. The ζ-potential was calculated from the electrophoretic mobility using the Smoluchowski relation.

III.2.5 Characterization of DNA capsules

The DNA capsules were observed at room temperature by confocal laser scanning microscopy (CLSM) with an FV1000-D (Olympus Corporation, Tokyo, Japan) equipped with an argon laser (488 nm) and laser diodes (559 and 635 nm). The

three-dimensional image of the capsules was rendered by using an ImageJ 1.42k (National Institutes of Health, Bethesda, MD). The enzymatic degradability of the DNA capsules was examined by immersing of the capsules into a 1 mg/ml (1,900 Kunitz units/ml) DNase I solution containing 100 mM $CaCl_2$, 100 mM $MgCl_2$, and 10 mM HEPES (pH 7.0). The degradation of the capsules was monitored by CLSM at room temperature. To test the permeability of the DNA capsules, the suspension of the capsules was mixed with FITC- or TRITC-dextran solutions (pH 7.0, containing 10 mM HEPES) and observed by CLSM after incubation for 12 h at room temperature. The surface morphology and the shell thickness of the DNA capsules were examined by atomic force microscopy (AFM) with an SPI3800N/SPA400 (SII NanoTechnology Inc., Chiba, Japan). AFM images were taken in dynamic force (cyclic contact) mode using a silicon cantilever with a spring constant of 38 N/m and a resonance frequency of 331 kHz. The samples were prepared by placing a drop of the suspension of the capsules onto a freshly cleaved mica surface and then drying in air.

III.3 Results and Discussion

In this study, porous $CaCO_3$ microparticles were employed as templates for the preparation of the DNA capsules. The porous structure of prepared $CaCO_3$ microparticles, which allows the infiltration of macromolecules into the templates, was confirmed by nitrogen adsorption–desorption measurement and FE-SEM. The pore size distribution of the $CaCO_3$ microparticles is shown in Fig. III.1. The average pore size and the BET surface area were 16 nm and 22 m^2/g, respectively. The diameter of $CaCO_3$ microparticles estimated from FE-SEM images was 4.2 ± 0.5 μm (mean value ± SD, n = 100 particles). The obtained $CaCO_3$ particles had smaller pore sizes and diameters than the reported values [32]. This is likely due to slight differences in the preparation

conditions, e.g., the mixing manner and the reaction time. The surface morphology of the uncoated $CaCO_3$ microparticles was shown in Fig. III.2A. Although a rough and granular porous surface was observed, this morphology was not appreciably changed even after the second coating and the third coating (Fig. III.2B and C). This result is reasonable considering that a few adsorption steps with polyelectrolytes cannot fill the pores of $CaCO_3$ microparticles unless their molecular weights are sufficiently high [26].

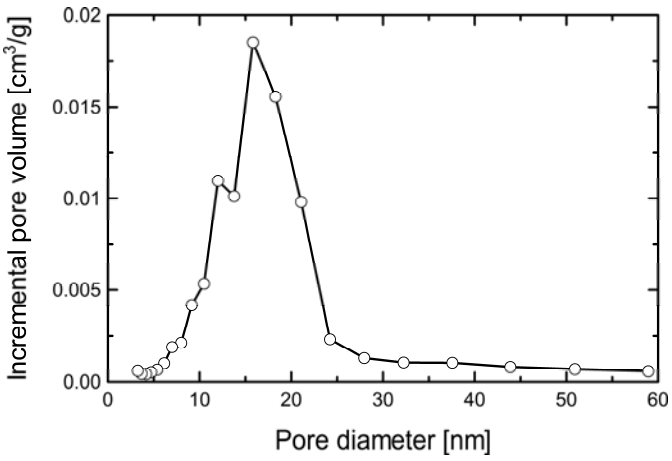

Figure III.1. Pore size distribution of uncoated $CaCO_3$ microparticles.

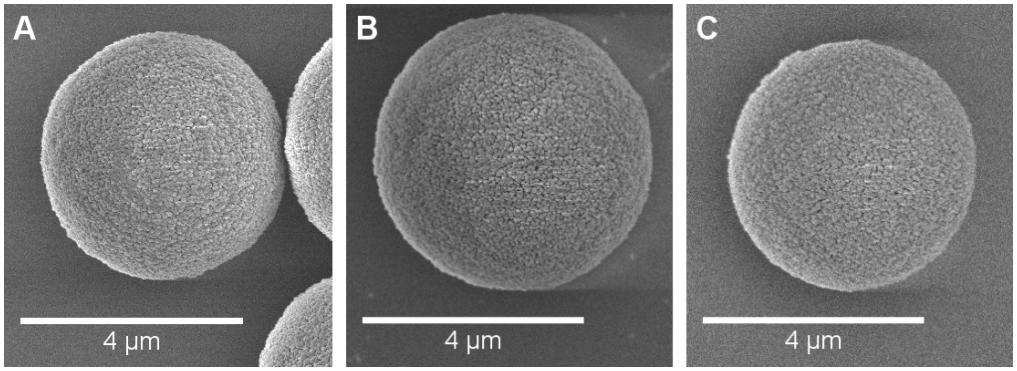

Figure III.2. FE-SEM images of an uncoated $CaCO_3$ microparticle (A) and DNA-adsorbed $CaCO_3$ microparticles after the second coating (B) and after the third coating (C). DNA strands were cross-linked with EGDE–TEMED.

We selected EGDE as the cross-linking agent to covalently link DNA strands. It is known that epoxy groups react with nucleophilic amino, hydroxyl, and sulfhydryl groups [33]; thus, EGDE would react with the amino groups of DNA bases under alkaline conditions, and leads to the cross-linking of DNA molecules. Previously, cross-linked DNA hydrogels with EGDE have been reported in many groups [34–36]. We performed the DNA cross-linking at room temperature, even though elevated temperatures accelerate the cross-linking reaction of epoxy groups [37,38]. This is because the $CaCO_3$ microparticles were unstable and recrystallized to microcrystals in water as reported previously [24], and even more unstable at high temperatures.

Fig. III.3A shows the CLSM images of the DNA-adsorbed $CaCO_3$ microparticles after cross-linking with EGDE–TEMED and the hollow DNA capsules obtained just after the addition of EDTA solution. The DNA strands were predominantly adsorbed onto the external surface of the $CaCO_3$ microparticles (Fig. III.3A; a, c, and e). By adding EDTA, the $CaCO_3$ microparticles were decomposed, resulting in cross-linked capsules comprised of DNA (Fig. III.3A; b, d, and f). The decomposition of the templates was observed from the transmission images. Without the cross-linking, the DNA strands were dissolved simultaneously with the templates in the EDTA solution. Fig. III.3B shows a three dimensional fluorescence image of the DNA capsules. The resulting hollow DNA capsules retained the spherical shape of the templates in the solution, without collapsing of the capsules.

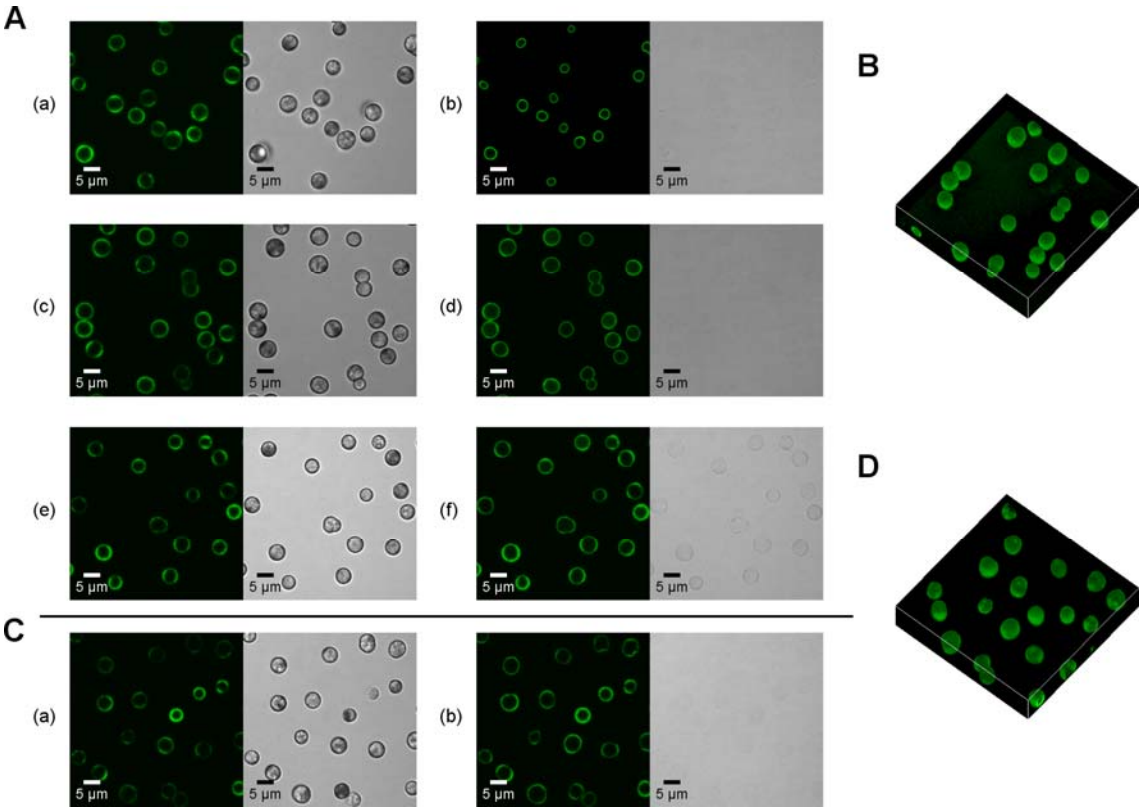

Figure III.3. (A) Fluorescence and transmission images of DNA-adsorbed $CaCO_3$ microparticles after the first coating and cross-linking with EGDE–TEMED (a, b), after the second coating (c, d), and after the third coating (e, f); and the images before (a, c, e) and just after (b, d, f) the addition of EDTA solution. (B) Three-dimensional image of DNA capsules with the second coating, DNA_2(TEMED). (C) Fluorescence and transmission images of DNA-adsorbed $CaCO_3$ microparticles after the first coating and cross-linking with EGDE–NaOH (a) and just after the addition of EDTA solution (b). (D) Three-dimensional image of DNA_1(NaOH) capsules. For the dissolution of the templates, DNA-adsorbed $CaCO_3$ microparticles (0.05% solids) were exposed to a 0.025 M EDTA solution. DNA was labeled with SYBR® Green II (Molecular Probes, Inc., Eugene, OR).

The DNA capsules without the additional coating had smaller diameters than those with the second or third coating (Fig. III.3A; b, d, and f). In considering this result, it should be noted that TEMED was used as an additive for the cross-linking reaction. When NaOH was used instead of TEMED, DNA adsorbed on $CaCO_3$ microparticles was not sufficiently cross-linked. (The initial pH of the cross-linking reaction was adjusted to 9.5 by the additives, i.e. NaOH or TEMED, in each case.) From the above results, we considered that TEMED would react with EGDE, and may connect the epoxy groups of EGDE that reacted with DNA strands. In other words, TEMED may act not only as a pH-adjusting agent but also as a second cross-linking agent. Topuz and Okay reported that the quaternization reaction of TEMED with EGDE occurs in the preparation of cross-linked DNA hydrogels [35]. Therefore, after the cross-linking with EGDE–TEMED, the DNA-adsorbed $CaCO_3$ microparticles bore a positive charge due to quaternary ammonium groups. This positive charge allowed the additional adsorption of DNA. The presence of positive charges was proved by ζ-potential measurements (Fig. III.4). In fact, the negative surface charges provided by DNA were inverted by the cross-linking with EGDE–TEMED. Without the additional coating, the quaternary ammonium groups would interact with the phosphate groups of the cross-linked DNA after the decomposition of the templates. We conjecture that this electrostatic attraction made the capsules shrink. In contrast, DNA adsorbed in the additional coating step compensated the positive charge of the quaternary ammonium groups, so that the shrinkage of the capsules with the second or third coating did not occur.

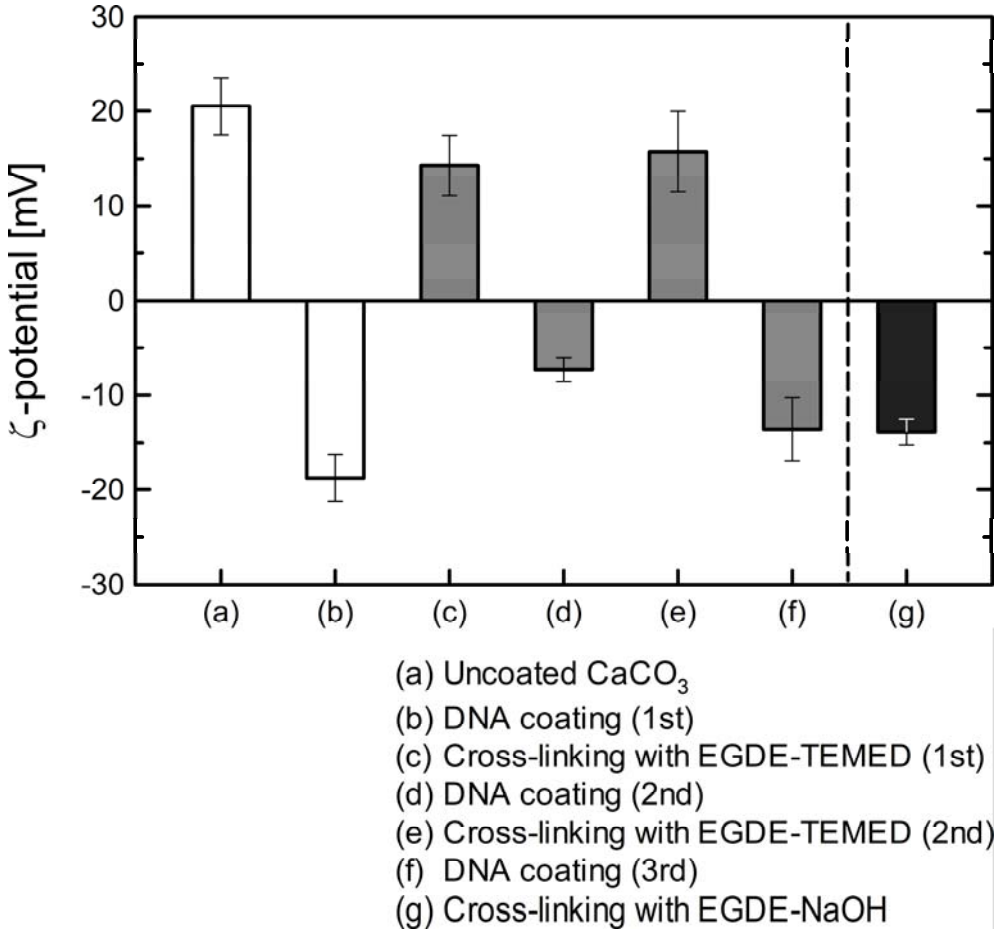

Figure III.4. ζ-potential of $CaCO_3$ microparticles after DNA adsorption and after the cross-linking with EGDE–TEMED and EGDE–NaOH. Each value is the mean ± SD of five replicates.

The cross-linking with EGDE–TEMED allows the consecutive adsorption of DNA via electrostatic interaction. By taking into account the reaction of TEMED with EGDE in the bulk solution, however, it was possible that the reaction between TEMED and EGDE produced quaternary ammonium polycations and that the resultant polycations could be adsorbed onto the DNA-adsorbed $CaCO_3$ microparticles, rendering the surfaces of DNA-adsorbed $CaCO_3$ microparticles positive. In this case, the resultant

DNA capsules can not be classified as single-component capsules in a precise sense because of polycations derived from TEMED and EGDE. To prepare single-component DNA capsules, we performed the cross-linking of DNA with 10 mM NaOH instead of 100 mM TEMED. CLSM images in Figs. 3C and D showed that hollow cross-linked DNA capsules were obtained without collapsing after the addition of EDTA solution. From ζ-potential measurements (Fig. III.4), the charge inversion, as observed after the cross-linking with EGDE–TEMED, was not observed after the cross-linking with EGDE–NaOH. These results indicate that the resulting DNA capsules were cross-linked with only EGDE.

AFM images of the cross-linked DNA capsules, DNA_2(TEMED), DNA_3(TEMED), and DNA_1(NaOH), are shown in Fig. III.5. Each of dried DNA capsules was collapsed on the mica surface. In contrast to DNA_2(TEMED) and DNA_1(NaOH) capsules, which had a pancake-like shape without folds or creases, DNA_3(TEMED) capsules formed circular creases, which is probably due to their highly cross-linked shell. DNA_2(TEMED) capsules were thinner and flatter than DNA_1(NaOH) capsules, despite the additional DNA coating (Figs. 5A and C). The doubled shell thickness of DNA_3(TEMED) capsules was estimated to be 21 nm from the thinnest section of the dried capsules (Fig. III.5B, bottom). This thickness is comparable with that of five-layer hollow LbL capsules consisting of DNA/spermidine templated on melamine formaldehyde particles (ca. 15–20 nm) [15].

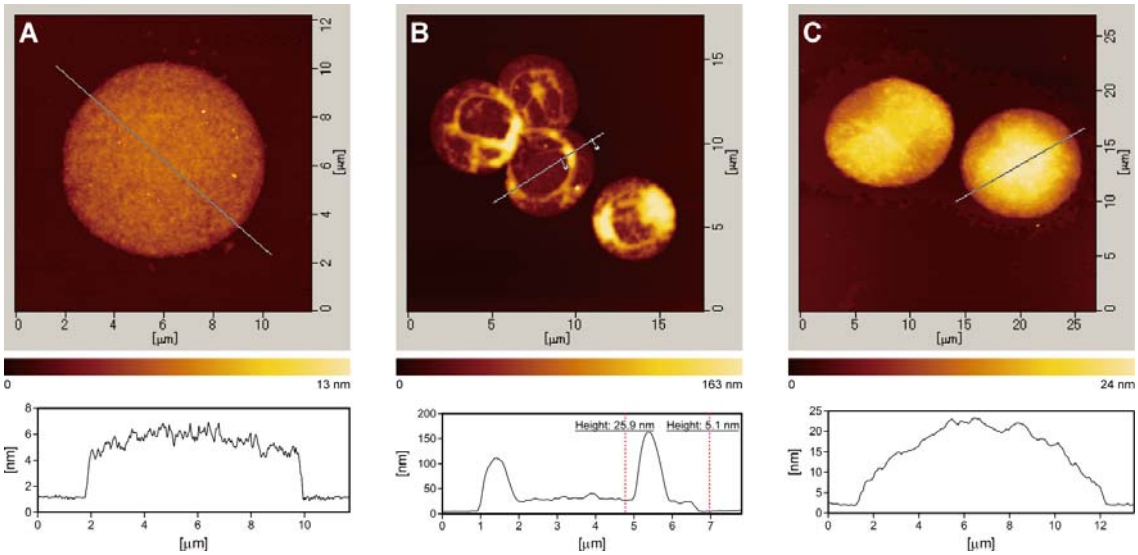

Figure III.5. AFM images of the DNA capsules and corresponding height profiles along the lines indicated in the AFM images: (A) DNA_2(TEMED), (B) DNA_3(TEMED), and (C) DNA_1(NaOH).

One of the advantages of a DNA capsule is biodegradability. In particular, a DNA capsule can be designed to be responsive to a variety of DNA-related enzymes. To evaluate the biodegradability of the DNA capsules prepared in the present study, the capsules were immersed in a DNase I solution. Fig. III.6 shows the enzymatic degradation of the DNA capsules. DNA_2(TEMED) capsules started to lose their capsular shape by 20-min immersion, and completely decomposed after 40 min (Fig. III.6A1). This decomposition was not observed in a DNase-free divalent salt solution for 24 h (Fig. III.6A2). DNA_3(TEMED) and DNA_1(NaOH) capsules immersed in the DNase I solution, however, did not decompose even after 6 h (Fig. III.6B and C, respectively). These results demonstrate that the DNA shell will be accessible for DNase I only if the extent of chemical cross-linking of DNA is sufficiently low. In this experiment, DNA_1(NaOH) capsules shrunk to a diameter of about 1.5 µm that is smaller

than the capsules in Fig. III.3C. This is presumably due to the high concentration of divalent metal ions (100 mM Ca^{2+} and 100 mM Mg^{2+}) required for the DNase-catalyzed reaction. The shrinkage of the DNA capsules would be caused by osmotic deswelling and by divalent-ion-induced DNA compaction similarly to what has been reported for DNA hydrogels [36]. Thus, when DNA_1(NaOH) capsules were placed in aqueous solutions without any additional salt, the capsules swelled to a diameter of around 8 μm (see CLSM images in Fig. III.7C below). In addition, we found that the degree of shrinkage of DNA_2(TEMED) and DNA_3(TEMED) capsules induced by ionic strength were lower than that of DNA_1(NaOH) (Fig. III.6A and B, respectively). This low shrinkage is likely because the electrostatic complexes in the DNA shell inhibited the uptake of divalent ions.

The permeability of a capsule is of major relevance for future applications such as encapsulation and drug delivery. We inspected the permeability behavior of the DNA capsules by CLSM. Fig. III.7 shows the CLSM images of the capsules after incubation in FITC- or TRITC-dextran solutions for 12 h. DNA_3(TEMED) capsules excluded FITC-dextran with a molecular weight of 250,000 (Fig. III.7A1), while they were completely permeable for low molecular weight TRITC-dextran (Mr ≈ 4,400) (Fig. III.7A2). In contrast, DNA_2(TEMED) and DNA_1(NaOH) capsules were completely permeable for high molecular weight FITC-dextran (Mr ≈ 2,000,000) (Fig. III.7B and C, respectively). The corresponding plots in Fig. III.7 clearly show the equal fluorescence intensity inside and outside each DNA capsule, except in the case of DNA_3(TEMED) capsules mixed with FITC-dextran (Mr ≈ 250,000). For some DNA_3(TEMED) capsules (approximately 10%, based on 300 capsules counted), the complete permeation of FITC-dextran was observed (indicated by the arrow in Fig. III.7A), probably indicating

incomplete cross-linking and the defects in the DNA shell. These results indicate that only highly cross-linked DNA capsules exhibited size-dependent permeability as well as that of hollow polyelectrolyte capsules prepared by LbL methods [19,39].

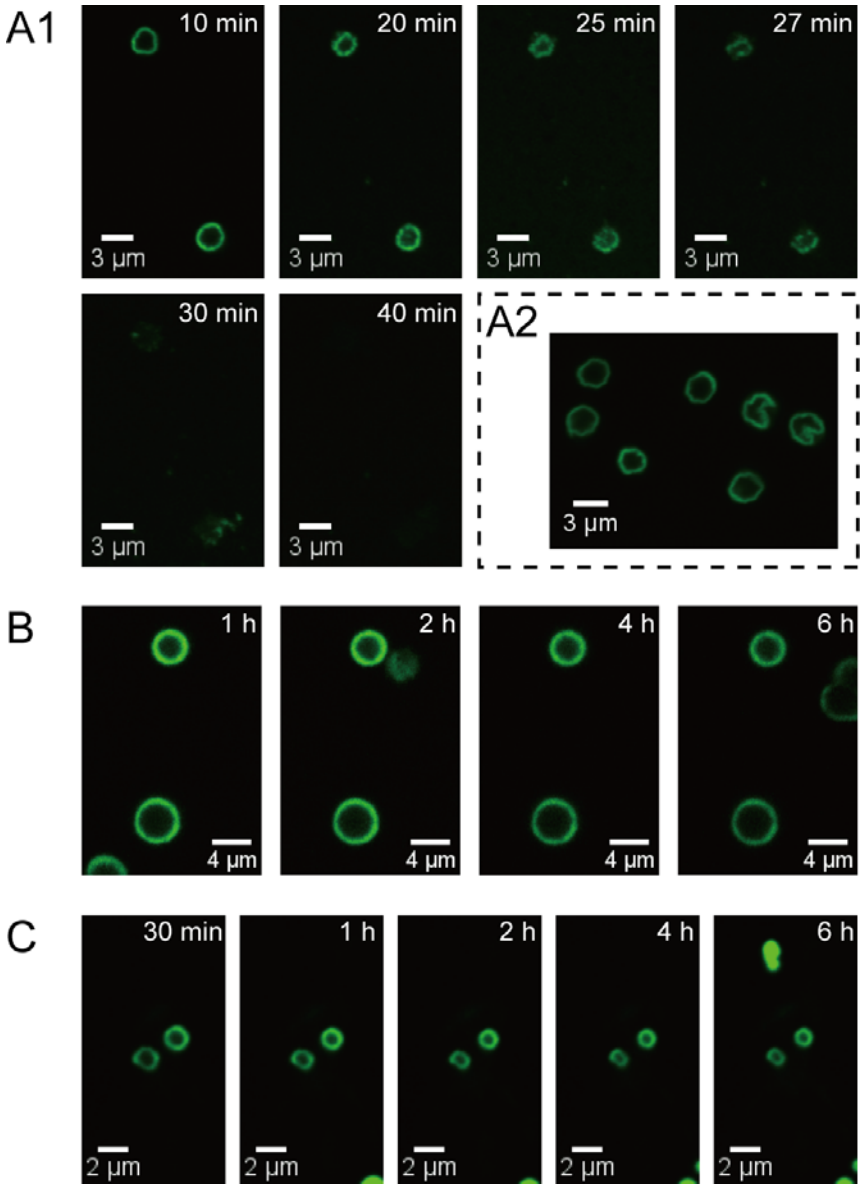

Figure III.6. CLSM images of DNA_2(TEMED) (A1), DNA_3(TEMED) (B), and DNA_1(NaOH) capsules (C) during immersion in a DNase I solution and of DNA_2(TEMED) capsules after 24-h immersion in a DNase-free divalent salt solution containing 100 mM $CaCl_2$ and 100 mM $MgCl_2$ (A2).

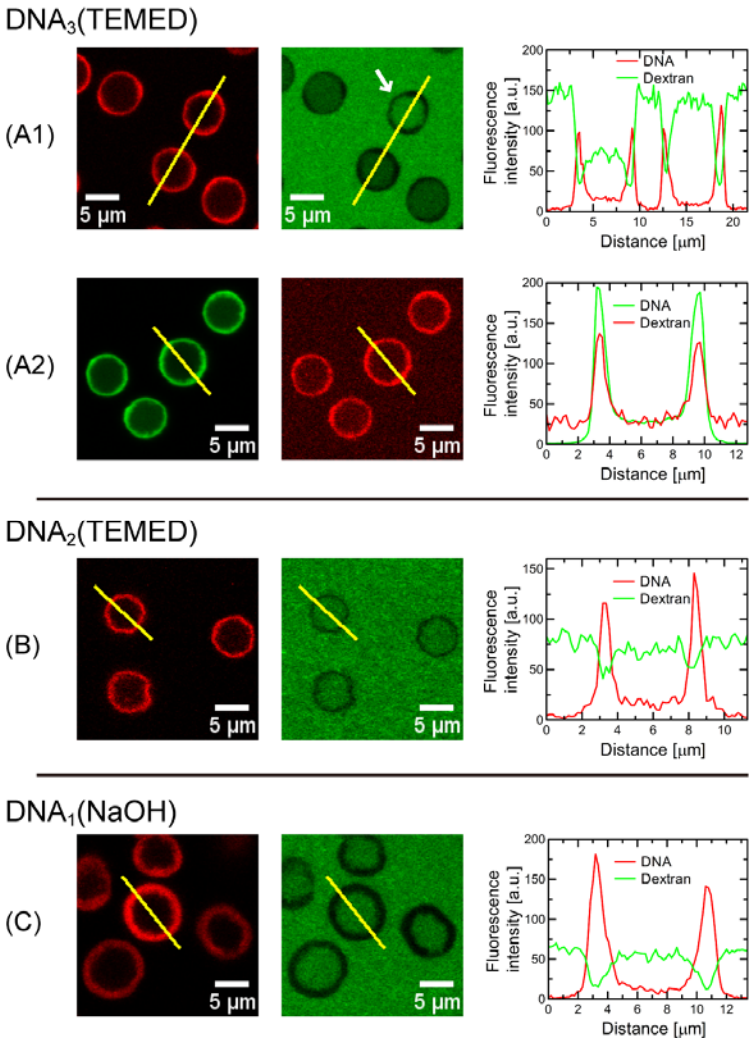

Figure III.7. CLSM images of DNA capsules after incubation in 0.5 mg/ml FITC- or TRITC-dextran solutions of different molecular weights for 12 h: DNA_3(TEMED) capsules mixed with FITC-dextran (*M*r ≈ 250,000) (A1), DNA_3(TEMED) capsules mixed with TRITC-dextran (*M*r ≈ 4,400) (A2), DNA_2(TEMED) capsules mixed with FITC-dextran (*M*r ≈ 2,000,000) (B), and DNA_1(NaOH) capsules mixed with FITC-dextran (*M*r ≈ 2,000,000) (C). DNA was labeled with TOTO®-3 (Molecular Probes, Inc., Eugene, OR) or SYBR® Green II. The arrow in (A1) indicates the capsules, which were completely permeable for FITC-dextran. The line graphs show the fluorescence intensity profiles along the yellow lines indicated in the CLSM images.

III.4 Conclusion

In this study, we developed a method for the preparation of cross-linked DNA capsules by using porous $CaCO_3$ microparticles as sacrificial templates. By using this method, three types of DNA capsules were prepared. Single-component DNA capsules were obtained by a single adsorption of DNA and by the subsequent cross-linking with EGDE and NaOH. The low cross-linked DNA capsules exhibited the enzymatic degradability. The size-dependent permeability of macromolecules through the highly cross-linked DNA capsules will be utilized as a compartmentalized microreactor and an encapsulation carrier. This templating method would be applicable to a wide range of other polyelectrolytes by reacting with a suitable cross-linking agent. We expect that this method will be useful to prepare single-component polymer capsules. Toward potential applications in biology and medicine, encapsulating drugs and chemicals in the capsules will be explored in the future.

References

[1] A. Kishimura, S. Liamsuwan, H. Matsuda, W.F. Dong, K. Osada, Y. Yamasaki, K. Kataoka, pH-dependent permeability change and reversible structural transition of PEGylated polyion complex vesicles (PICsomes) in aqueous media, Soft Matter 5 (2009) 529–532.

[2] O. Kreft, A.M. Javier, G.B. Sukhorukov, W.J. Parak, Polymer microcapsules as mobile local pH-sensors, J. Mater. Chem. 17 (2007) 4471–4476.

[3] D. Lensen, D.M. Vriezema, J.C.M. van Hest, Polymeric microcapsules for synthetic applications, Macromol. Biosci. 8 (2008) 991–1005.

[4] M. Kobašlija, D.T. McQuade, Polyurea microcapsules from oil-in-oil emulsions via interfacial polymerization, Macromolecules 39 (2006) 6371–6375.

[5] H.N. Yow, A.F. Routh, Formation of liquid core–polymer shell microcapsules, Soft Matter 2 (2006) 940–949.

[6] W. Meier, Polymer nanocapsules, Chem. Soc. Rev. 29 (2000) 295–303.

[7] G. Decher, Fuzzy nanoassemblies: toward layered polymeric multicomposites, Science 277 (1997) 1232–1237.

[8] C.S. Peyratout, L. Dähne, Tailor-made polyelectrolyte microcapsules: from multilayers to smart containers, Angew. Chem. Int. Ed. 43 (2004) 3762–3783.

[9] W. Tong, C. Gao, Multilayer microcapsules with tailored structures for bio-related applications, J. Mater. Chem. 18 (2008) 3799–3812.

[10] K. Glinel, G.B. Sukhorukov, H. Möhwald, V. Khrenov, K. Tauer, Thermosensitive hollow capsules based on thermoresponsive polyelectrolytes, Macromol. Chem. Phys. 204 (2003) 1784–1790.

[11] B.G. De Geest, A.M. Jonas, J. Demeester, S.C. De Smedt, Glucose-responsive

polyelectrolyte capsules, Langmuir 22 (2006) 5070–5074.

[12] M.F. Bédard, B.G. De Geest, A.G. Skirtach, H. Möhwald, G.B. Sukhorukov, Polymeric microcapsules with light responsive properties for encapsulation and release, Adv. Colloid Interface Sci., in press.

[13] B.G. De Geest, A.G. Skirtach, A.A. Mamedov, A.A. Antipov, N.A. Kotov, S.C. De Smedt, G.B. Sukhorukov, Ultrasound-triggered release from multilayered capsules, Small 3 (2007) 804–808.

[14] Y. Itoh, M. Matsusaki, T. Kida, M. Akashi, Enzyme-responsive release of encapsulated proteins from biodegradable hollow capsules, Biomacromolecules 7 (2006) 2715–2718.

[15] C. Schüler, F. Caruso, Decomposable hollow biopolymer-based capsules, Biomacromolecules 2 (2001) 921–926.

[16] C.R. Kinnane, G.K. Such, G. Antequera-García, Y. Yan, S.J. Dodds, L.M. Liz-Marzan, F. Caruso, Low-fouling poly(*N*-vinyl pyrrolidone) capsules with engineered degradable properties, Biomacromolecules 10 (2009) 2839–2846.

[17] Y. Zhang, Y. Guan, S. Zhou, Single component chitosan hydrogel microcapsule from a layer-by-layer approach, Biomacromolecules 6 (2005) 2365–2369.

[18] A.N. Zelikin, Q. Li, F. Caruso, Disulfide-stabilized poly(methacrylic acid) capsules: formation, cross-Linking, and degradation behavior, Chem. Mater. 20 (2008) 2655–2661.

[19] W. Tong, C. Gao, H. Möhwald, Single polyelectrolyte microcapsules fabricated by glutaraldehyde-mediated covalent layer-by-layer assembly, Macromol. Rapid Commun. 27 (2006) 2078–2083.

[20] L. Duan, Q. He, X. Yan, Y. Cui, K. Wang, J. Li, Hemoglobin protein hollow shells

fabricated through covalent layer-by-layer technique, Biochem. Biophys. Res. Commun. 354 (2007) 357–362.

[21] L. Duan, W. Qi, X. Yan, Q. He, Y. Cui, K. Wang, D. Li, J. Li, Proton gradients produced by glucose oxidase microcapsules containing motor F_0F_1-ATPase for continuous ATP biosynthesis, J. Phys. Chem. B 113 (2009) 395–399.

[22] G.K. Such, E. Tjipto, A. Postma, A.P.R. Johnston, F. Caruso, Ultrathin, responsive polymer click capsules, Nano Lett. 7 (2007) 1706–1710.

[23] Y. Wang, V. Bansal, A.N. Zelikin, F. Caruso, Templated synthesis of single-component polymer capsules and their application in drug delivery, Nano Lett. 8 (2008) 1741–1745.

[24] D.V. Volodkin, N.I. Larionova, G.B. Sukhorukov, Protein encapsulation via porous $CaCO_3$ microparticles templating, Biomacromolecules 5 (2004) 1962–1972.

[25] A.I. Petrov, A.A. Antipov, G.B. Sukhorukov, Base-acid equilibria in polyelectrolyte systems: from weak polyelectrolytes to interpolyelectrolyte complexes and multilayered polyelectrolyte shells, Macromolecules 36 (2003) 10079–10086.

[26] A. Szarpak, I. Pignot-Paintrand, C. Nicolas, C. Picart, R. Auzély-Velty, Multilayer assembly of hyaluronic acid/poly(allylamine): control of the buildup for the production of hollow capsules, Langmuir 24 (2008) 9767–9774.

[27] S.H. Um, J.B. Lee, N. Park, S.Y. Kwon, C.C. Umbach, D. Luo, Enzyme-catalysed assembly of DNA hydrogel, Nat. Mater. 5 (2006) 797–801.

[28] X.D. Liu, H.Y. Diao, N. Nishi, Applied chemistry of natural DNA, Chem. Soc. Rev. 37 (2008) 2745–2757.

[29] N.K. Navani, Y. Li, Nucleic acid aptamers and enzymes as sensors, Curr. Opin. Chem. Biol. 10 (2006) 272–281.

[30] A.P.R. Johnston, H. Mitomo, E.S. Read, F. Caruso, Compositional and structural engineering of DNA multilayer films, Langmuir 22 (2006) 3251–3258.

[31] A.P.R. Johnston, F. Caruso, Stabilization of DNA multilayer films through oligonucleotide crosslinking, Small 4 (2008) 612–618.

[32] D.V. Volodkin, A.I. Petrov, M. Prevot, G.B. Sukhorukov, Matrix polyelectrolyte microcapsules: new system for macromolecule encapsulation, Langmuir 20 (2004) 3398–3406.

[33] G.T. Hermanson, Bioconjugate Techniques, second ed., Academic Press, London, 2008.

[34] T. Amiya, T. Tanaka, Phase transitions in cross-linked gels of natural polymers, Macromolecules 20 (1987) 1162–1164.

[35] F. Topuz, O. Okay, Formation of hydrogels by simultaneous denaturation and cross-linking of DNA, Biomacromolecules 10 (2009) 2652–2661.

[36] D. Costa, M.G. Miguel, B. Lindman, Effect of additives on swelling of covalent DNA gels, J. Phys. Chem. B 111 (2007) 8444–8452.

[37] L. Sundberg, J. Porath, Preparation of adsorbents for biospecific affinity chromatography I. attachment of group-containing ligands to insoluble polymers by means of bifuctional oxiranes, J. Chromatogr. 90 (1974) 87–98.

[38] H.W. Sung, C.S. Hsu, Y.S. Lee, D.S. Lin, Crosslinking characteristics of an epoxy-fixed porcine tendon: effects of pH, temperature, and fixative concentration, J. Biomed. Mater. Res. 31 (1996) 511–518.

[39] G. Berth, A. Voigt, H. Dautzenberg, E. Donath, H. Möhwald, Polyelectrolyte complexes and layer-by-layer capsules from chitosan/chitosan sulfate, Biomacromolecules 3 (2002) 579–590.

Chapter IV

Preparation of DNA hydrogel capsules cross-linked through NeutrAvidin–biotin interaction

IV.1 Introduction

Hollow spheres and capsules have attracted much attention for their diverse applications, including drug delivery, biosensing, bioimaging, and catalyst [1–5]. A variety of techniques to prepare capusles have been developed so far, for example chemical techniques such as interfacial polymerization and in-situ polymerization, and a physicochemical technique such as coacervation [6–8]. Capsules prepared by self-assembling of amphiphilic block copolymers and those of colloidal particles, which are known as polymersomes and colloidosomes, respectively, have been extensively investigated recently [9,10]. Among self-assembled species, polyelectrolyte multilayers formed by the layer-by-layer (LbL) method are available for the shell of hollow capsules by using colloidal particles as a sacrificial template [11]. As an attractive feature of this method, the shell thickness, dimensions, and functionalities of the LbL capsules can be controlled by the total numbers of layer deposited [12,13], the diameter of the templates [14], and the composition of the multilayers [13,15,16], respectively.

Wang et al. used mesoporous shell silica particles as templates and prepared thick-walled and single-component polymer nanocapsules [17]. In our previous study, we developed a method for the preparation of cross-linked single-component polyelectrolyte capsules by using porous calcium carbonate ($CaCO_3$) microparticles as templates [18]. These templating methods have a distinct advantage over the

conventional LbL method: a time-consuming sequential adsorption process is not necessary to obtain hollow polyelectrolyte capsules. In addition, the porous $CaCO_3$ microparticles used in our method can easily be dissolved under mild conditions with chelating agents, and can be coated or filled with various macromolecules (proteins, polysaccharides, nucleic acids, and other polyelectrolytes) [19–21]. Our method was applied to the preparation of covalently cross-linked DNA hydrogel capsules [18]. The adsorbed DNA strands in $CaCO_3$ microparticles were successfully cross-linked with a cross-linking agent, ethylene glycol diglycidyl ether. However, it takes a long time (24 h) to form the hollow capsules. Furthermore, the epoxy groups of the employed cross-linker will react readily with preloaded substances, such as drugs for encapsulation into $CaCO_3$ microparticles, and this reaction will result in the loss of biological activity of the substances.

To overcome the above disadvantages, in this work we propose a modified method for the preparation of cross-linked polyelectrolyte capsules by non-covalent cross-linking based on avidin-biotin interaction. The egg-white glycoprotein, avidin has four binding sites for a biotin molecule with a high affinity (binding constant ~ 10^{15} M^{-1}) [22,23]. Thus, by using avidin as a cross-linker, biotin-immobilized materials (nanoscale metal colloids and wires, and lipid vesicles) were bound to each other [24–27]. The successful preparation of LbL assemblies consisting of avidin and biotin-labeled polyamines was reported by Anzai et al. [28]. From these studies, it is likely that avidin can also cross-link the biotinylated polymers adsorbed in porous microparticles. To prepare DNA capsules, the biotin labeling of DNA is required for the cross-linking through avidin-biotin interaction. As a cross-linker, we adopted NeutrAvidin (NAv), the deglycosylated derivative of avidin, to avoid the electrostatic

interaction with DNA, because the isoelectric point (pI) of NAv is much lower than that of avidin [29,30]. At neutral pH, both DNA and NAv (pI = 6.3) have a net negative charge, while avidin (pI = 10.5) has a net positive charge.

The preparation procedure of the non-covalently cross-linked DNA cpasules is shown schematically in Scheme IV.1. First, biotin-labeled DNA was adsorbed into porous $CaCO_3$ microparticles. This is followed by the adsorption of NAv for the cross-linking of the adsorbed DNA. Then, the $CaCO_3$ microparticles are removed by the addition of a chelating agent. In this study, we prepared DNA capsules by two different procedures: one is the method described just above, and the other is the LbL method consisting of nine consecutive adsorption steps of DNA and NAv. The essential difference between the two methods is the total number of adsorption steps before the dissolution of $CaCO_3$ microparticles. Furthermore, we investigated the permeability of the prepared DNA capsules.

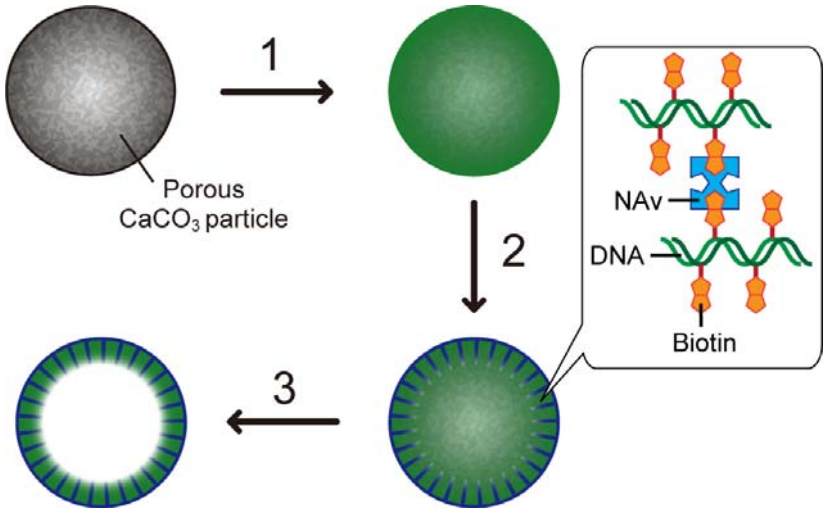

Scheme IV.1. Schematic illustration of the preparation process of the non-covalently cross-linked DNA capsules by using porous $CaCO_3$ microparticles as a template: adsorption of biotin-labeled DNA (step 1), cross-linking of DNA with the adsorption of NAv (step 2), and dissolution of $CaCO_3$ microparticles with chelating agent (step 3).

IV.2 Experimental section

IV.2.1 Materials

The sources of chemicals used were as follows: herring sperm DNA (*M*r ≈ 10,000–30,000, catalog no. D3159) was from Sigma–Aldrich (St. Louis, MO); NeutrAvidin (NAv) was from Thermo Fisher Scientific Inc. (Waltham, MA); sodium carbonate (Na_2CO_3), calcium chloride dihydrate ($CaCl_2 \cdot 2H_2O$), 1,6-diaminohexane, and *N*-bromosuccinimide (NBS) were from Wako Pure Chemical Industries (Osaka, Japan); ethylenediaminetetraacetic acid disodium salt dihydrate ($EDTA \cdot 2Na \cdot 2H_2O$) and ninhydrin reagent (catalog no. N7285) were from Sigma-Aldrich; 2-(4-Hydroxyphenylazo)benzoic acid (HABA) and biotin *N*-hydroxysuccinimide ester were from Tokyo Chemical Industry Co,.Ltd. (Tokyo, Japan); biotin and lipoic acid were from Wako Pure Chemical Industries; biotin hydrazide, 1-(3-dimethylaminopropyl)-3-ethylcarbodiimide hydrochloride (EDC), fluorescein isothiocyanate-dextran (FITC-dextran, *M*r ≈ 2,000,000), tetramethylrhodamine isothiocyanate-dextran (TRITC-dextran, *M*r ≈ 155,000), and TRITC-dextran (*M*r ≈ 56,000) were from Sigma-Aldrich; and HEPES, MES and Bicine were from Nacalai Tesque, Inc. (Kyoto, Japan). DNA was purified by phenol/chloroform extraction and ethanol precipitation with sodium acetate (0.3 M) before use. All of other reagents were used as received. The pure water used in all experiments was prepared with a Milli-Q® Integral water purification system (Millipore, Bedford, MA) and had a resistivity of 18.2 MΩ·cm. The concentration of DNA and NAv were determined by using an extinction coefficient of 20 at 260 nm for a 1mg/ml DNA solution and an extinction coefficient of 1.66 at 280 nm for a 1mg/ml NAv solution, respectively.

IV.2.2 Preparation of porous $CaCO_3$ microparticles

$CaCO_3$ microparticles were prepared according to Volodkin et al [31]. In brief, 0.33 M Na_2CO_3 aqueous solution (100 ml) was rapidly poured into an equal volume of 0.33 M $CaCl_2$ solution under vigorous stirring (1000 rpm), and the mixture was stirred for 30 s at 25°C. After the mixing, the resultant suspension was left without stirring for 3 min and then was diluted in 2 l of pure water. The precipitates of $CaCO_3$ microparticles were collected and washed on glass fiber filters (150 mm diameter, GF/D; Whatman International Ltd., Maidstone, UK) by vacuum filtration, and then were dried under vaccum at room temperature.

IV.2.3 Biotin labeling of DNA

Before the treatment of DNA with a biotin-labeling reagent, which can react with primary amines, aminated DNA was prepared in the following manner as described in the literature [32]. A herring sperm DNA solution (10 mg/ml in 0.1 M sodium bicarbonate; 1.5 ml) was mixed with an NBS solution (8 mM in water; 14.2 ml) and was incubated for 10 min in an ice–water bath. Immediately after this step, a 1,6-diaminohexane solution (750 mM in water; 9.1 ml) was added to the brominated DNA solution. The mixture was heated to 50°C for 1 h. To remove excess diamine, the DNA solution was concentrated to approximately 0.5 ml with 1-butanol, and the aminated DNA was isolated by repeated ethanol precipitation. For the biotinylation of DNA, a biotin *N*-hydroxysuccinimide ester solution (10 mg/ml in dimethyl sulfoxide; 1.5 ml) was added to an aminated DNA solution (0.5 mg/ml in 100 mM Bicine buffer, pH 8.5; 15 ml), and the mixture was kept at room temperature for 1 h. Finally, the biotin-labeled DNA was concentrated by butanol extraction and was collected by

repeated ethanol precipitation.

To measure the amount of amine groups and biotin molecules of the biotin-labeled DNA, we used the ninhydrin assay [33] and the HABA assay [23,34], respectively. In the ninhydrin assay, the ninhydrin reagent (200 μl) was added to the DNA solution (0.3 mg/ml in 10 mM acetic acid; 400 μl). After the mixed solution was boiled to 100°C for 10 min, the solution was cooled to room temperature. The resulting purple-colored solution (540 μl) was diluted with ethanol (900 μl) before absorbance measurement with a spectrophotometer (V-630; JASCO, Tokyo, Japan). The observed absorbance values at 570 nm were used to calculate the amount of amine groups with known concentrations of 1,6-diaminohexane as standard. For the HABA assay, an HABA–NAv complex solution was prepared by the adding of a stock solution of HABA (10 mM HABA in 10 mM NaOH; 90 μl) to a quartz cuvette (final volume: 2.4 ml) containing 0.5 mg/ml of NAv in phosphate buffer (100 mM phosphate, 150 mM NaCl, pH 7.4). The decrease in absorbance at 500 nm was recorded with the spectrophotometer equipped with a magnetic stirrer and a temperature controller (EHC-716; JASCO) after the addition of the biotin-labeled DNA solution (1 mg/ml in pure water; 20 μl) to the cuvette. The amount of biotin present in the DNA solution was determined with a calibration curve obtained by sequential addition of 25 μl of biotin solution (0.14 mg/ml in pure water) to a cuvette containing the NAv–HABA complex solution. In this assay, the absorbance at 500 nm was measured under constant stirring at 20°C after reaching a constant value, and these values were corrected for the dilution caused by the addition of the biotin-containing solutions.

IV.2.4 Preparation of DNA capsules

The DNA capsules prepared by two consecutive adsorption steps and the LbL method are designated as $(DNA/NAv)_1$ and $DNA/(NAv/DNA)_4$ capsules, respectively. For the preparation of $(DNA/NAv)_1$ capsules, the adsorption of the two components was performed as follows. An aqueous suspension of $CaCO_3$ microparticles (10% w/v; 10 μl) was mixed with a biotin-labeled DNA solution (2 mg/ml in 10 mM HEPES buffer, pH 7.0; 90 μl). The mixture was incubated for 30 min at room temperature with gentle shaking. To remove excess DNA, the $CaCO_3$ microparticles were washed five times with pure water by centrifugation at 1000 × *g* for 30s. DNA-adsorbed $CaCO_3$ microparticles (10% w/v; 10 μl) were then added to an NAv solution (2 mg/ml; 90 μl) in phosphate buffer (10 mM phosphate, 100 mM NaCl, pH 7.0). The $CaCO_3$ microparticles were incubated and washed as described above. In the case of LbL-coated $DNA/(NAv/DNA)_4$ capsules, $CaCO_3$ microparticles were coated alternately nine times with DNA and NAv in the same manner as above. To remove the $CaCO_3$ templates, a 0.2 M EDTA solution (50 μl) was added to the suspension of the $CaCO_3$ microparticles (1% w/v; 50 μl). Obtained DNA capsules were purified by a 1-h dialysis against pure water using Slide-A-Lyzer MINI Dialysis units (20,000 MWCO; Pierce, Rockford, IL).

IV.2.5 Field-emission scanning electron microscopy (FE-SEM)

The surface morphology of the DNA-adsorbed $CaCO_3$ microparticles was observed by FE-SEM (JSM-7500F; JEOL Ltd., Tokyo, Japan) operating at an accelerating voltage of 5 kV. The samples were prepared by placing a drop of the suspension of the $CaCO_3$ microparticles onto a double-sided adhesive tape attached to a sample holder. After

lyophilizing the samples, they were sputter-coated with Pt/Pd.

IV.2.6 Quartz crystal microbalance (QCM) analysis

The adsorption of the biotin-labeled DNA and NAv and the buildup of the LbL assembly were followed in situ with a QCM (Q-Sense E1; Biolin Scientific, Västra Frölunda, Sweden) equipped with a flow chamber. In this experiment, Au-coated quartz crystals were used and cleaned with piranha solution (concentrated H_2SO_4/30% H_2O_2 in a volume ratio of 3:1). *Caution: piranha solution reacts violently with organic materials and should not be stored in closed containers.* For the biotin modification of the Au-surface prior to the measurements, the quartz crystals were immersed in a lipoic acid solution (1 mg/ml in ethanol) for 24 h to introduce carboxyl groups on the surface [35]. After rinsing with water, the crystals were treated for 12 h with a biotin hydrazide solution (4 mM in 90 mM MES buffer, pH 4.7) containing 4 mM EDC. The biotin-functionalized quartz crystals were washed and then were set in the chamber, where the temperature was maintained at 25 °C. NAv (0.1 mg/ml) and DNA (0.1 mg/ml) solutions, which were prepared in phosphate buffer (10 mM phosphate, 100 mM NaCl, pH 7.0), were alternately injected to the chamber at a flow rate of 30 µl/min. After the saturated adsorption of the two components, the chamber was rinsed with the same buffer before adding the next solution. In this paper, the frequency shift of the ninth overtone (≈ 45 MHz) of the quartz crystal was used for analysis.

IV.2.7 Confocal laser scanning microscopy (CLSM)

The DNA capules and the DNA-adsorbed $CaCO_3$ microparticles were observed at room temperature by CLSM with an FV1000-D (Olympus Corporation, Tokyo, Japan)

equipped with laser diodes (473 nm and 635 nm) and a He-Ne laser (543 nm). The permeability of the DNA capsules was examined by immersing of the capsules into FITC- or TRITC-dextran solutions (0.5 mg/ml in water) at room temperature. At a given incubation time, CLSM images were taken at the equatorial plane of the capsules.

IV.3 Results and Discussion

For the preparation of DNA capsules by our method, the synthesis of biotin-labeled DNA is necessary. We preliminarily prepared aminated DNA so that biotin molecules can bind to DNA through the reaction of primary amine groups with the succinimidyl ester of the biotin-labeling reagent. The degree of biotinylation was determined by the HABA assay. It is known that HABA binds with lower affinity to avidin than biotin does, and shifts its color from yellow to red due to charge-transfer complex formation [36]. Therefore, adding biotin-conjugated molecules to an avidin–HABA complex solution leads the decrease of the absorbance at 500 nm because of biotin displaces HABA. The amount of amine groups, which was determined by ninhydrin assay, and that of biotin molecules bound to the modified DNA are summarized in Table IV.1. It was found that unreacted amine groups remain in the resulting DNA. From the decrease of the amine groups after the biotinylation reaction, the biotinylation degree, the number of biotin molecules bound per 100 base pairs of DNA, was estimated to be 66 molecules. However, the biotinylation degree measured directly by the HABA assay was only 30 molecules. This low value is probably because the HABA assay only detects active biotin that is able to interact with avidin without steric hindrance. The amount of biotin bound to the DNA can be controlled by the concentration of NBS used during the preparation of the aminated DNA. In the case of the biotin-labeled DNA prepared with

0.8 mM instead of the normal 8 mM NBS concentration, the biotinylation degree was decreased to 7 molecules (Table IV.1).

Table IV.1. The amination degree and biotinylation degree of the modified DNA

NBS concentration	Aminated DNA	Biotin-labeled DNA	
	Amine[a]	Amine[a]	Biotin[a]
8 mM	95.1 ± 3.0	28.6 ± 1.3	29.8 ± 1.7
0.8 mM	19.8 ± 0.9	4.9 ± 0.4	6.8 ± 0.7

[a] The number of groups or molecules bound per 100 base pairs of DNA

The porous structure of $CaCO_3$ microparticles would allow for the infiltration of DNA and NAv into the templates. Fig. IV.1 shows the surface morphology of the DNA/NAv-adsorbed and the uncoated $CaCO_3$ microparticles. The granular and porous surface of the uncoated surface remained unchanged after the two adsorption steps (Fig. IV.1A and B). In contrast, the surface pores of LbL-coated $CaCO_3$ microparticles that were used to prepare DNA/$(NAv/DNA)_4$ capsules were not observed (Fig. IV.1C). This indicates that the surface of the micropaticles was fully covered with a DNA/NAv assembly. The presence of the adsorbed DNA and NAv in the microparticles was confirmed by CLSM. Fig. IV.2 shows the CLSM images of the DNA/NAv-adsorbed $CaCO_3$ microparticles and the images of the same area taken just after the addition of EDTA solution. The biotin-labeled DNA was adsorbed throughout the interior of the microparticles, presumably owing to its low molecular weight, whereas NAv did not penetrate to the center of the microparticles (Fig. IV.2a,c, and e). The DNA strands presented around the center of the microparticles were not cross-linked with NAv, so that upon the template dissolution by adding EDTA, hollow $(DNA/NAv)_1$ capsules were obtained (Fig. IV.2b). As can be seen from the fluorescence image of capsules, two

fluorescence colors were observed in the shell of the capsules (red and green), which indicates that the shell was comprised of DNA and NAv. In our previous method using covalent cross-linking [18], sufficiently high molecular weight of DNA, which was adsorbed near the external surface of the $CaCO_3$ microparticles, was required to yield hollow structures of cross-linked DNA strands. Thus, it was found that our approach in this study makes it possible to prepare hollow DNA capsules even when a small size of DNA is employed. The DNA/$(NAv/DNA)_4$ capsules were successfully prepared by LbL method as shown in Fig. IV.2d. However, by using the DNA with low degree of biotinylation, well-shaped hollow $(DNA/NAv)_1$ capsules was not observed (Fig. IV.2f). In this case, weakly cross-linking of the DNA resulted in deformed and unstable capsules that were too fragile to withstand the stress during the purification step to remove EDTA.

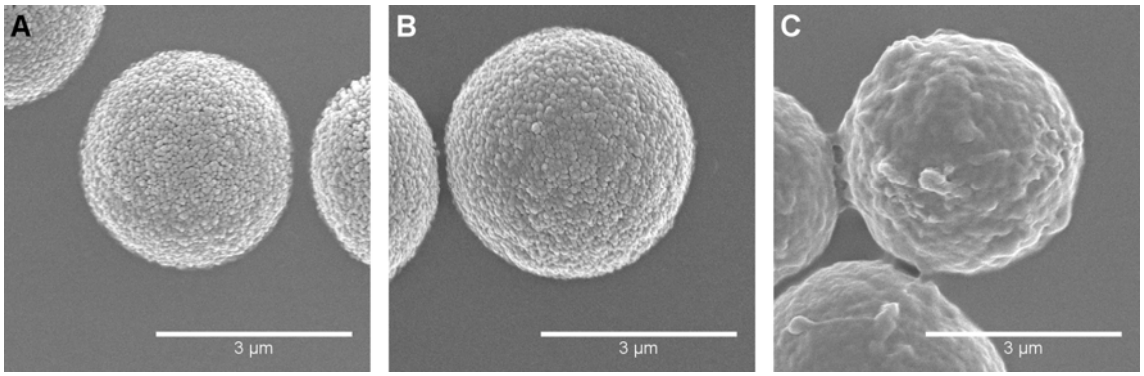

Figure IV.1. FE-SEM images of an uncaoted $CaCO_3$ microparticle (A) and DNA/NAv adsorbed $CaCO_3$ microparticles after the two adsorption steps (B) and after the nine consecutive adsorption steps (C).

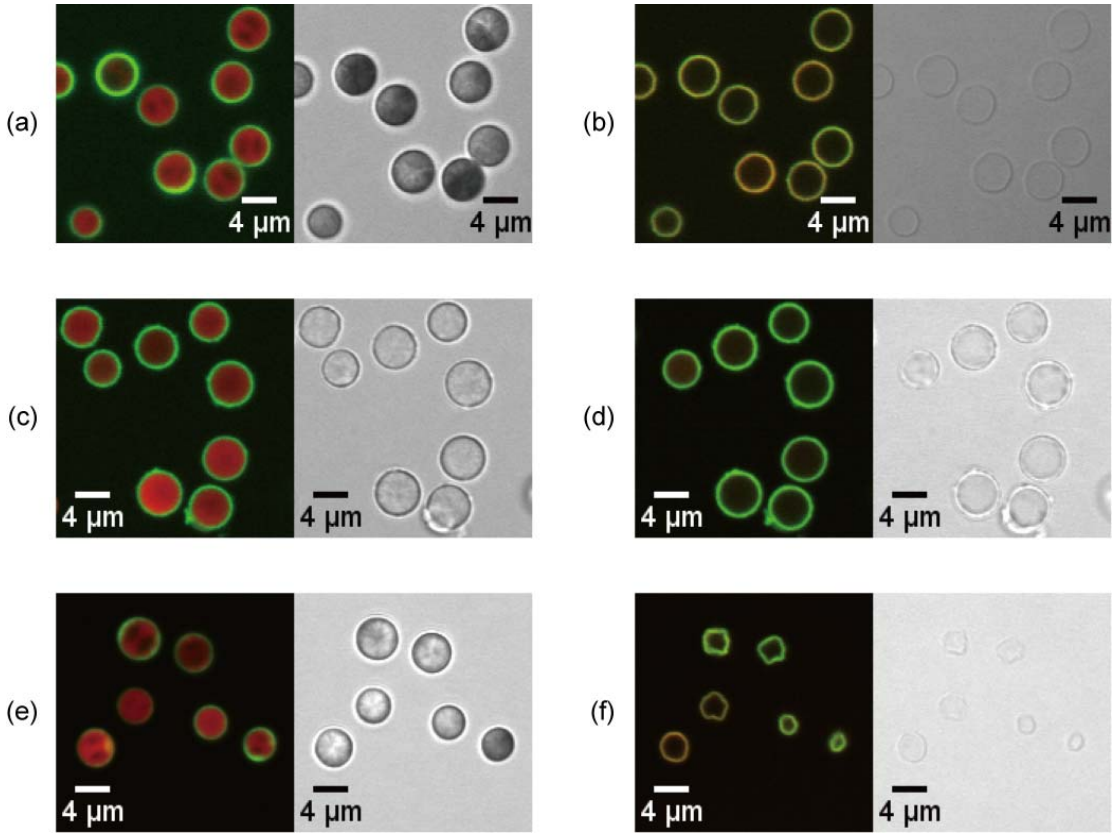

Figure IV.2. Fluorescence and transmission images of DNA/NAv-adsorbed $CaCO_3$ microparticles before (a, c, and e) and just after (b, d, and f) the addition of EDTA solution: (a, b) $(DNA/NAv)_1$ coating, (c, d) $DNA(NAv/DNA)_4$ coating, and (e, f) $(DNA/NAv)_1$ coating with DNA with low biotinylation degree. DNA was labeled with TOTO®-3 (red; Molecular Probes, Inc., Eugene, OR), and NAv was visualized by adding biotin-4-fluorescein (green; Invitrogen, Carlsbad, CA).

The bulidup of LbL assembly consisting of biotin-labeled DNA and NAv on a planar surface was monitored by QCM. For the measurement, the surface of quartz crystals, being coated with biotin, were initially deposited with NAv. A representative frequency

change in the QCM measurement is plotted in Fig. IV.3. A reduction in the frequency means that the adsorption from flowing solutions was occurred on the crystals. The stepwise decrease in the frequency revealed the successful assembly of DNA/NAv multilayers. The fequency shifts upon the adsorption of NAv were significantly larger than that upon the adsorption of biotin-labeled DNA. This is reasonable considering that the high degree of biotinylation of the DNA as shown above in Table IV.1. Although covalently cross-linked DNA capsules and LbL assemblies containing DNA can be decomposed by adding deoxyribonuclease [18,37], the removal of the DNA/NAv multilayers from the crystals was not detected as a decrease in the frequency during an enzymatic treatment with deoxyribonuclease I. This is probably due to the modification of DNA with a high degree. To maintain the biodegradability of DNA/NAv capsules, the improvement of the biotinylation of DNA will be addressed in future work.

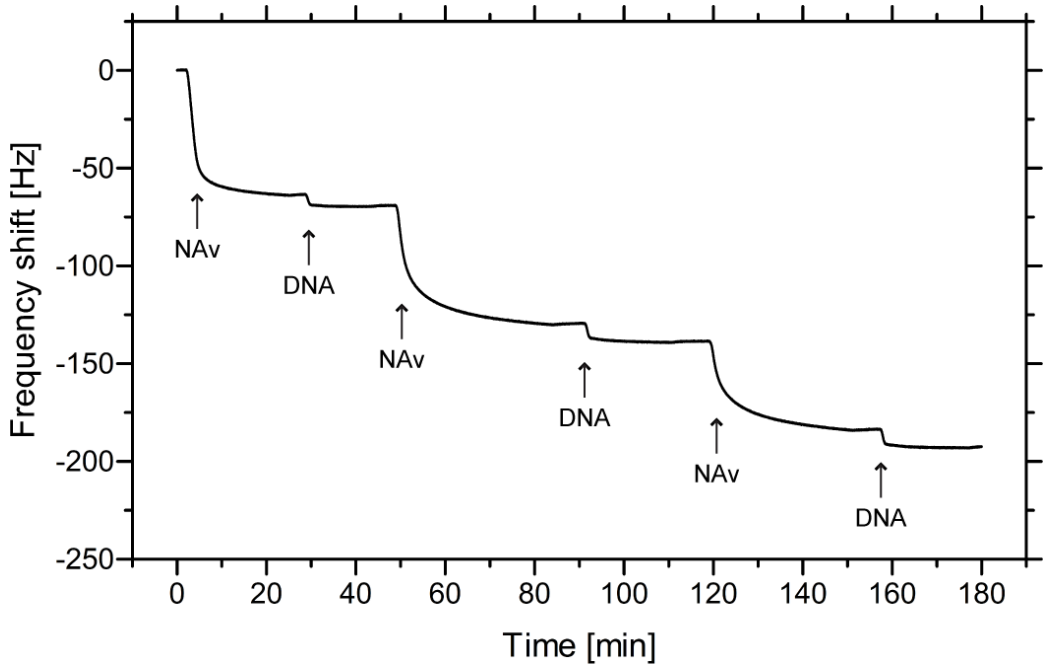

Figure IV.3. Change in QCM frequency following the addition of NAv and biotin-labeled DNA.

Finally, we studied the capsule permeability, which relates to potential applications requiring encapsulation of macromolecules. Fig. IV.4 shows the CLSM images of the DNA/(NAv/DNA)$_4$ capsules after incubation in FITC- or TRITC-dextran solutions for 15 h. The distribution of the fluorescence inside the capsules suggests the permeation of the fluorescent dextran through the DNA/NAv shells. The DNA/(NAv/DNA)$_4$ capsules were completely permeable for TRITC-dextran with a molecular weight of 56,000 (Fig. IV.4A), while they excluded high molecular weight dextrans (Mr ≈ 155,000 and 2,000,000) (Fig. IV.4B and C). These results demonstrate that the DNA/NAv capsules prepared by LbL method based on avidin–biotin interaction exhibited size-dependent permeability. Both methods used in this study yielded hollow DNA capsules such as (DNA/NAv)$_1$ and DNA/(NAv/DNA)$_4$ capsules; however, the (DNA/NAv)$_1$ shells did not act as a barrier against the penetration of high molecular weight dextrans. Judging from the FE-SEM images shown in Fig. IV.1, compared with the DNA/NAv-adsorbed $CaCO_3$ microparticles, the LbL-coated micropartcles were completely covered with the assemblies. The (DNA/NAv)$_1$ capsules may have defects in the shells because the assemblies prepared by the two adsorption steps would be formed exclusively inside the pores of the $CaCO_3$ microparticles. The $CaCO_3$ crystals that support the assemblies will be converted to large pores in the shells after the template dissolution. The DNA/(NAv/DNA)$_4$ capsules possess additional layers on the top of the shells, and probably thereby has the inherent permeability of the DNA/NAv multilayers.

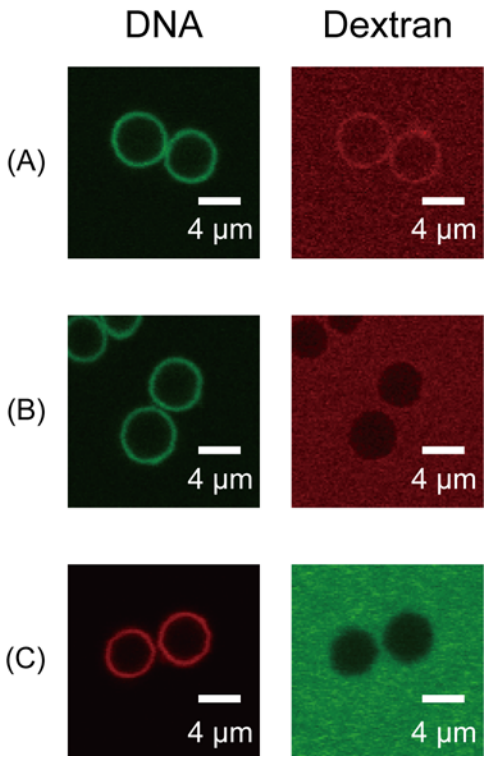

Figure IV.4. CLSM images of DNA/(NAv/DNA)$_4$ capsules after incubation in 0.5 mg/ml FITC- or TRITC-dextran solutions of different molecular weight for 15 h: DNA capsules labeled green with SYBR® Green I (Molecular Probes, Inc., Eugene, OR) in the TRITC-dextran (red; *M*r ≈ 56,000) solution (A), DNA capsules labeled green with SYBR® Green I in the TRITC-dextran (red; *M*r ≈ 155,000) solution (B), and DNA capsules labeled red with TOTO®-3 in the FITC-dextran (green; *M*r ≈ 2,000,000) solution (C).

IV.4 Conclusion

Non-covalently cross-linked DNA capsules with the shell formed by NeutrAvidin–biotin interaction, were successfully prepared by our templating method. The (DNA/NAv)$_1$ capsules, obtained after the two adsorption steps of biotin-labeled

DNA and NAv, could be prepared with a significantly shorter cross-linking time (30 min) as compared with covalently cross-linked DNA capsules prepared by our previous method (24 h). By using these two components, LbL multilayers could be assembled as proved by the QCM measurements, and LbL-coated capsules were also prepared. In the case of the LbL-coated DNA/(NAv/DNA)$_4$ capsules, selective permeability of macromolecules through the capsules was observed. We consider that this templating method would be applicable to various polymers that can be adsorbed into porous templates, although the biotinylation of the polymers is indispensable. The future goal of this research is to provide the encapsulation of low molecular weight compounds so that our method will become more useful to prepare hollow polymer capsules for biological and biomedical applications.

References

[1] L. Yang, P. Alexandridis, Physicochemical aspects of drug delivery and release from polymer-based colloids, Curr. Opin. Colloid Interface Sci. 5 (2000) 132–143.

[2] L.J. De Cock, S. De Koker, B.G. De Geest, J. Grooten, C. Vervaet, J.P. Remon, G.B. Sukhorukov, M.N. Antipina, Polymeric multilayer capsules in drug delivery, Angew. Chem. Int. Ed. 49 (2010) 2–22.

[3] S. Chinnayelka, M.J. McShane, Microcapsule biosensors using competitive binding resonance energy transfer assays based on apoenzymes, Anal. Chem. 77 (2005) 5501–5511.

[4] G.B. Sukhorukov, A.L. Rogach, B. Zebli, T. Liedl, A.G. Skirtach, K. Köhler, A.A. Antipov, N. Gaponik, A.S. Susha, M. Winterhalter, W.J. Parak, Nanoengineered polymer capsules: tools for detection, controlled delivery, and site-specific manipulation, Small 1 (2005) 194–200.

[5] D. Lensen, D.M. Vriezema, J.C.M. van Hest, Polymeric microcapsules for synthetic applications, Macromol. Biosci. 8 (2008) 991–1005.

[6] J. Cui, Y. Wang, A. Postma, J. Hao, L. Hosta-Rigau, F. Caruso, Monodisperse polymer capsules: tailoring size, shell thickness, and hydrophobic cargo loading via emulsion templating, Adv. Funct. Mater. 20 (2010) 1625–1631.

[7] R. Qiao, X.L. Zhang, R. Qiu, Y.S. Kang, Synthesis of functional microcapsules by in situ polymerization for electrophoretic image display elements, Colloids Surf. A 313–314 (2008) 347–350.

[8] J. Lazko, Y. Popineau, J. Legrand, Soy glycinin microcapsules by simple coacervation method, Colloids Surf. B 37 (2004) 1–8.

[9] D.E. Discher, F. Ahmed, Polymersomes, Annu. Rev. Biomed. Eng. 8 (2006)

323–341.

[10] F.J. Rossier-Miranda, C.G.P.H. Schroën, R.M. Boom, Colloidosomes: versatile microcapsules in perspective, Colloids Surf. A 343 (2009) 43–49.

[11] C.S. Peyratout, L. Dähne, Tailor-made polyelectrolyte microcapsules: from multilayers to smart containers, Angew. Chem. Int. Ed. 43 (2004) 3762–3783.

[12] G.B. Sukhorukov, E. Donath, H. Lichtenfeld, E. Knippel, M. Knippel, A. Budde, H. Möhwald, Layer-by-layer self assembly of polyelectrolytes on colloidal particles, Colloids Surf. A 137 (1998) 253–266.

[13] K. Glinel, G.B. Sukhorukov, H. Möhwald, V. Khrenov, K. Tauer, Thermosensitive hollow capsules based on thermoresponsive polyelectrolytes, Macromol. Chem. Phys. 204 (2003) 1784–1790.

[14] H. Zhu, E.W. Stein, Z. Lu, Y.M. Lvov, M.J. McShane, Synthesis of size-controlled monodisperse manganese carbonate microparticles as templates for uniform polyelectrolyte microcapsule formation, Chem. Mater. 17 (2005) 2323–2328.

[15] W. Qi, X. Yan, L. Duan, Y. Cui, Y. Yang, J. Li, Glucose-sensitive microcapsules from glutaraldehyde cross-linked hemoglobin and glucose oxidase, Biomacromolecules 10 (2009) 1212–1216.

[16] S. Erokhina, L. Benassi, P. Bianchini, A. Diaspro, V. Erokhin, M.P. Fontana, Light-driven release from polymeric microcapsules functionalized with bacteriorhodopsin, J. Am. Chem. Soc. 131 (2009) 9800–9804.

[17] Y. Wang, V. Bansal, A.N. Zelikin, F. Caruso, Templated synthesis of single-component polymer capsules and their application in drug delivery, Nano Lett. 8 (2008) 1741–1745.

[18] A. Fujii, T. Maruyama, Y. Ohmukai, E. Kamio, T. Sotani, H. Matsuyama,

Cross-linked DNA capsules templated on porous calcium carbonate microparticles, Colloids Surf. A 356 (2010) 126–133.

[19] D.V. Volodkin, N.I. Larionova, G.B. Sukhorukov, Protein encapsulation via porous $CaCO_3$ microparticles templating, Biomacromolecules 5 (2004) 1962–1972.

[20] Z. Wang, L. Qian, X. Wang, F. Yang, X. Yang, Construction of hollow DNA/PLL microcapsule as a dual carrier for controlled delivery of DNA and drug, Colloids Surf. A 326 (2008) 29–36.

[21] G.B. Sukhorukov, D.V. Volodkin, A.M. Günther, A.I. Petrov, D.B. Shenoy, H. Möhwald, Porous calcium carbonate microparticles as templates for encapsulation of bioactive compounds, J. Mater. Chem. 14 (2004) 2073–2081.

[22] N.M. Green, Avidin and streptavidin, Methods Enzymol. 184 (1990) 51–67.

[23] N.M. Green, Spectrophotometric determination of avidin and biotin, Methods Enzymol. 18 (1970) 418–424.

[24] S. Mann, W. Shenton, M. Li, S. Connolly, D. Fitzmaurice, Biologically programmed nanoparticle assembly, Adv. Mater. 12 (2000) 147–150.

[25] K.K. Caswell, J.N. Wilson, U.H.F. Bunz, C.J. Murphy, Preferential end-to-end assembly of gold nanorods by biotin–streptavidin connectors, J. Am. Chem. Soc. 125 (2003) 13914–13915.

[26] A.K. Salem, M. Chen, J. Hayden, K.W. Leong, P.C. Searson, Directed assembly of multisegment Au/Pt/Au nanowires, Nano Lett. 4 (2004) 1163–1165.

[27] S. Chiruvolu, S. Walker, J. Israelachvili, F.J. Schmitt, D. Leckband, J.A. Zasadzinski, Higher order self-assembly of vesicles by site-specific binding, Science 264 (1994) 1753–1756.

[28] J. Anzai, Y. Kobayashi, N. Nakamura, M. Nishimura, T. Hoshi, Layer-by-layer

construction of multilayer thin films composed of avidin and biotin-labeled poly(amine)s, Langmuir 15 (1999) 221–226.

[29] Y. Hiller, J.M. Gershoni, E.A. Bayer, M. Wilchek, Biotin binding to avidin. Oligosaccharide side chain not required for ligand association, Biochem. J. 248 (1987) 167–171.

[30] I.B.R. Ramírez, L. Ekblad, B. Jergil, Affinity partitioning of biotinylated mixed liposomes: effect of charge on biotin–NeutrAvidin interaction, J. Chromatogr. B 743 (2000) 389–396.

[31] D.V. Volodkin, A.I. Petrov, M. Prevot, G.B. Sukhorukov, Matrix polyelectrolyte microcapsules: new system for macromolecule encapsulation, Langmuir 20 (2004) 3398–3406.

[32] G.T. Hermanson, Bioconjugate Techniques, second ed., Academic Press, London, 2008.

[33] M. Friedman, Applications of the ninhydrin reaction for analysis of amino acids, peptides, and proteins to agricultural and biomedical sciences, J. Agric. Food Chem. 52 (2004) 385–406.

[34] N.M. Green, A spectrophotometric assay for avidin and biotin based on binding of dyes by avidin, Biochem. J. 94 (1965) 23c–24c.

[35] Q. Cheng, A.B. Toth, Permselectivity, sensitivity, and amperometric pH sensing at thioctic acid monolayer microelectrodes, Anal. Chem. 68 (1996) 4180–4185.

[36] O. Livnah, E.A. Bayer, M. Wilchek, J.L. Sussman, The structure of the complex between avidin and the dye, 2-(4'-hydroxyazobenzene) benzoic acid (HABA), FEBS lett. 328 (1993) 165168.

[37] T. Serizawa, M. Yamaguchi, M. Akashi, Time-controlled desorption of ultrathin

polymer films triggered by enzymatic degradation, Angew. Chem. Int. Ed. 42 (2003) 1115–1118.

Chapter V

General Conclusion

Functional polyelectrolyte microparticles and microcapsules were successfully prepared by using two kinds of core materials, such as anionic microgels and porous calcium carbonate ($CaCO_3$) microparticles, and these polyelectrolyte microspheres were characterized. In the both cases of the substrates, hydrogel microspheres can be obtained by the methods described in this work. After the layer-by-layer (LbL) deposition, microgels coated with polyelectrolytes turned into core-shell type microgels. By using another method in which $CaCO_3$ microparticles were used as sacrificial templates, cross-linked hollow hydrogel microcapsules were prepared. Although the resulting hydrogel microspheres by these methods were prepared from existing materials, the altered responsive behavior of microgels and the preparation of previously unreported hollow microcapsules were achieved. Thus, by using these methods, it is possible to prepare novel capsules that are suitable for a particular application. The obtained insights in this study would provide fundamental understanding to prepare functional capsules with a novel behavior and would contribute to prepare various hydrogel capsules consisted of biomaterials.

The conclusions of this work are summarized as follows:

1. pH-responsive Behavior of Hydrogel Microspheres Altered by Layer-by-layer Assembly of Polyelectrolytes

Polyelectrolyte coating to pH-responsive microgels by the LbL method formed

multilayer shells on the surface of the microgels and influenced their pH-responsive changes in the size. In addition, it was found that pH-response of the microgels can be controlled by the type of polyelectrolytes adsorbed. In brief, the molecular weight of adsorbing polyelectrolytes is a major factor affecting the pH-responsive behavior. Polycations, which are smaller than the mesh size of substrate anionic microgels, diffused into the microgels and formed complex with the chain of anionic gels. The swelling of the microgels as a function of pH is governed by the charge balance in the complex between the adsorbed polyelectrolytes and the ionic groups of microgels. Therefore, the isoelectric point of adsorbing weak polyelectrolytes will be important to control the pH-response. In contrast, in the case of sufficiently high molecular weight chitosan, the resultant microgels maintained nearly the same pH-response as the original microgel. These findings also prove the wide applicability of LbL method because polyelectrolyte assemblies not only coat pH-responsive microgels but also modify their behavior.

2. Cross-linked DNA capsules templated on porous calcium carbonate microparticles

In this study, novel templating method was developed based on the LbL method. The traditional LbL method requires at least two components and a prolonged preparation time owing to the sequential adsorption of components. In contrast, by using this templating method, single-component polymer capsules can be prepared. The key features of this method are the single adsorption of a single component into porous templates and the following chemical cross-linking of the adsorbed components. By using this method, resultant hollow native DNA microcapsules, which have not been

prepared so far, exhibited enzymatic degradability and size-dependent permeability of macromolecules, according to the cross-linking conditions. This technique has the potential to be used for the preparation of various polymer capsules and provide a facile approach differing from the traditional LbL method.

3. Preparation DNA hydrogel capsules cross-linked through NeutrAvidin–biotin interaction

The successful preparation of single-component native DNA capsules was achieved by the novel method described above. However, one of the problems associated with the traditional LbL method still remained because the chemical cross-linking of the adsrobed DNA is also time-consuming. To improve this method, the covalent cross-linking procedure was changed to the manner without using any cross-linking agents for DNA. In this modified method, NeutrAvidin molecules act as a cross-linker for biotin-labeled DNA. As a result, non-covalent cross-linking technique through avidin–biotin actually accelerated the cross-linking procedure. Because biotinylation can be applied to different macromolecules, the wide applicability of developed templating method in this study would be maintained. In addition, the combination biotin-labeled DNA and NeutrAvidin could be applied to layer-by-layer assembled multilayers.

List of Publications

Chapter II **pH-responsive Behavior of Hydrogel Microspheres Altered by Layer-by-layer Assembly of Polyelectrolytes,** **Akihiro Fujii**, Tatsuo Maruyama, Tomohiro Sotani, Yoshikage Ohmukai, Hideto Matsuyama, Colloids Surf. A 337 (2009) 159–163.

Chapter III **Cross-linked DNA capsules templated on porous calcium carbonate microparticles,** **Akihiro Fujii**, Tatsuo Maruyama, Yoshikage Ohmukai, Eiji Kamio, Tomohiro Sotani, Hideto Matsuyama, Colloids Surf. A 356 (2010) 126–133.

Chapter IV **Preparation of DNA hydrogel capsules cross-linked through NeutrAvidin–biotin interaction,** **Akihiro Fujii**, Yoshikage Ohmukai, Tatsuo Maruyama, Tomohiro Sotani, Hideto Matsuyama, submitted to Colloids Surf. A.

Other Publications

Preparation of monodispersed polyelectrolyte microcapsules with high encapsulation efficiency by an electrospray technique, Yu Fukui, Tatsuo Maruyama, Yuko Iwamatsu, **Akihiro Fujii**, Tsutomu Tanaka, Yoshikage Ohmukai, Hideto Matsuyama, Colloids Surf. A 370 (2010) 28–34.